**ALMA MATER STUDIORUM - UNIVERSITÀ DI BOLOGNA**

SCUOLA DI INGEGNERIA

DIPARTIMENTO di
INGEGNERIA DELL'ENERGIA ELETTRICA E DELL'INFORMAZIONE
"Guglielmo Marconi"
DEI

**CORSO DI LAUREA IN INGEGNERIA DELL'AUTOMAZIONE**
**CURRICULUM: AUTOMATION ENGINEERING**

---

**TESI DI LAUREA**
in
*Controlli Automatici T-2*

# Modelling and Control of a 2-D version of a Ball-Balancing Robot

CANDIDATO

*Gioele Buriani*

RELATORE

*Chiar.mo Prof. Lorenzo Marconi*

CORRELATORE

*Ing. Mario Spirito*

Anno Accademico
*2020/2021*

Sessione
*I*

ALMA MATER STUDIORUM

# *Abstract*

Department of Electrical, Electronic, and Information Engineering "Guglielmo Marconi" - DEI

Bachelor degree in Automation Engineering

**Modelling and control of a 2-D version of a Ball-Balancing Robot**

by Gioele BURIANI

Il Ball-Balancing Robot è un innovativo modello di robot in grado di muoversi liberamente sul piano rimanendo in equilibrio su una sfera. Lo scopo di questa tesi è la modellazione e il controllo di una versione 2-D semplificata di questo robot, formata sostanzialmente da una ruota che tende a rimanere in equilibrio su un cilindro. Ciò permette migliore conoscenza del funzionamento di questo robot e getta le basi per una futura realizzazione pratica della versione 3-D.

La prima parte della tesi si concentra sulla modellazione del sistema. Dapprima vengono considerate tutte le dinamiche che si presentano al contatto fra ruota e cilindro, prevalentemente legate alle varie forme di attrito fra i due corpi. In seguito, questa analisi viene applicata ad un caso più simile alla realtà in cui si tiene conto della forza di gravità e di un piano su cui il sistema può spostarsi.

La seconda parte del lavoro mira invece alla creazione di un sistema di controllo che permetta, applicando una determinata coppia alla ruota, sia di tenerla in equilibrio, sia di spostare il sistema a una distanza prestabilita. In particolare viene implementato prima il controllo di posizione assumendo un caso ideale in cui il robot rimane stabile, mirando ad ottenere una risposta relativamente veloce e, soprattutto, precisa. La seconda parte del controllo verte invece sul problema della stabilizzazione del sistema, cercando di mantenere la ruota al di sopra del cilindro a fronte di incertezze iniziali.

Dato che questo progetto è soltanto una parte di un obbiettivo più complesso, nella parte finale vengono poi suggeriti alcuni possibili sviluppi futuri per ampliare e arricchire il lavoro che puntano al raggiungimento della realizzazione finale del robot in 3-D.

Keywords: Ball-Balancing Robot, pure rolling, sliding, state-space control

# *Acknowledgements*

I would like to express my deep sense of gratitude towards Engineer Mario Spirito, my supervisor for this work, that has always been able to guide me and to provide me with fast and precise answers to my doubts, while always keeping a friendly and reassuring attitude.

It is also my pleasure to thank Professor Nicola Sancisi who, although I have not been a direct student of his, has shown immense kindness and availability to help me solve a problem I got stuck in.

Last but not least, I would like to thank my dear friend and colleague Edoardo Panichi for the technical advice and the material he provided me with during my work.

# Contents

**Abstract** iii

**Acknowledgements** v

**1 Introduction** 1

**2 Modelling** 5
2.1 Introduction . . . 5
2.2 Rolling with fixed rotation axis . . . 5
2.2.1 Linear analysis of dry friction . . . 6
2.2.2 Rolling behaviour . . . 7
2.2.3 Rolling friction . . . 8
2.2.4 Conditions recap . . . 9
2.2.5 Dynamical model with fixed axes . . . 10
2.2.6 Presence of a load . . . 12
2.2.7 Final equations . . . 13
2.2.8 Additional considerations . . . 13
2.2.9 Conclusion . . . 14
2.3 Rolling with moving rotation axis . . . 14
2.3.1 Change due to relative rotation . . . 15
2.3.2 Change due to linear motion . . . 17
2.3.3 Final $\alpha$ expression . . . 18
2.3.4 Final $N$ calculation . . . 18
2.3.5 Tangential component of the weight . . . 19
2.3.6 Torque generated by the normal component of the weight . . . 20
2.3.7 Final equations for the system . . . 21

**3 Control** 23
3.1 Introduction . . . 23
3.2 Control for the fixed axes case . . . 23
3.2.1 Transfer function for the fixed axes case . . . 23
3.2.2 Controller design for the fixed axes case . . . 27
Definition of the specifics . . . 27
Stabilization of the system with static gain . . . 28
Implementation of anticipatory networks . . . 29
Implementation of a prefilter . . . 31
3.2.3 Implementation on real system for the fixed axes case . . . 33
Addition of an integrator . . . 33
Elimination of the settling tail . . . 34
3.2.4 Presence of a load . . . 35
3.2.5 Saturation of the control input . . . 37
Definition and application of the saturation . . . 37
Implementation of an anti-windup network . . . 40

3.3 Control for the moving axes case . . . 41
3.3.1 State space representation of the moving axes case . . . 41
Rearrangement of the dynamics equations with state variables 42
Linearization of the system . . . 43
3.3.2 Controller design for the moving axes case . . . 46
Stability analysis of the autonomous case . . . 46
Pole placement . . . 47
LQR . . . 49
3.3.3 Implementation on real system for the moving axes case . . . 50
LQR implementation . . . 50
Input variable considerations . . . 52
3.3.4 Implementation of saturation . . . 53
3.3.5 Integration of the steady state error . . . 55

**4 Future Developments** **59**
4.1 Introduction . . . 59
4.2 Optimization . . . 59
4.2.1 Carter's analysis on micro slip . . . 59
4.2.2 Rolling with sliding with the ground . . . 60
4.2.3 Other modelling optimizations . . . 60
4.2.4 Optimization of the controllers . . . 60
4.3 Expansion . . . 60
4.3.1 Addition of an inverted pendulum . . . 60
4.3.2 Modelling of the motor . . . 62
4.3.3 Combination of the two controls . . . 63
4.3.4 Expansion to the 3-D case . . . 63

**5 Conclusion** **65**

**Bibliography** **67**

# List of Figures

1.1 The first Ball-Balancing Robot built at Carnegie Mellon University, USA in 2005 . . . 1
1.2 A later version of ball-Balancing Robot built at ETH Zurich, Switzerland in 2010 . . . 2
1.3 Droid BB-8, from the Star Wars cinematic universe . . . 3

2.1 Linear analysis of static dry friction . . . 6
2.2 Linear analysis of dynamic dry friction . . . 7
2.3 Diagram showing the principle behind rolling friction . . . 8
2.4 A 2D overview of the considered system . . . 10
2.5 The system with the addition of the load torque $C_L$ . . . 12
2.6 A 2D overview of the considered system . . . 14
2.7 The geometrical representation of $a$ . . . 15
2.8 The geometrical representation of $d$ and $d_0$ as seen from the bottom cylinder . . . 17
2.9 The geometrical construction to find $W_{1tc}$ . . . 19
2.10 The geometrical construction to find $C_{W_{1n}}$ . . . 20

3.1 The bode diagram of the system with only $R(s) = -1$ . . . 28
3.2 The step response of the closed loop system with only $R(s) = -1$ . . . 28
3.3 The bode diagram of L(s) . . . 30
3.4 The step response of F(s) . . . 31
3.5 The value of $u$ in time after a step input of 1 . . . 31
3.6 The Simulink configuration of the system . . . 32
3.7 The values of $u$ in time for the prefiltered system after a step input of 1 32
3.8 The step response of the final system . . . 33
3.9 The step response of the real system with respect to the reference . . . 33
3.10 The step response of the real system with respect to the reference after adding an integrator . . . 34
3.11 The final step response of the real system with respect to the reference 35
3.12 The final control input to the system with a step reference of 1m . . . 35
3.13 The step response of the system with a positive load of 10Nm . . . 36
3.14 The step response of the system with a negative load of -10Nm . . . 36
3.15 The control input to the system with a positive load of 10Nm . . . 37
3.16 The control input to the system with a negative load of -10Nm . . . 37
3.17 The control input to the system with a reference of 5m and no load with saturation . . . 38
3.18 The step response of the system with a reference of 5m and no load with saturation . . . 39
3.19 The control input to the system with a reference of 10m and no load with saturation . . . 39
3.20 The step response of the system with a reference of 10m and no load with saturation . . . 40

3.21 The control input to the system with a reference of 10m and no load with the anti-windup network . . . 40
3.22 The step response of the system with a reference of 10m and no load with the anti-windup network . . . 41
3.23 The Simulink configuration of the final control scheme for the fixed axes case . . . 41
3.24 The value of $d$ and $\alpha$ for $\theta_{10} = \frac{\pi}{10}$ . . . 47
3.25 The response of the system for $\theta_{10} = \frac{\pi}{10}$ with the implementation of the first matrix $K$ by pole placement . . . 48
3.26 The response of the system for $\theta_{10} = \frac{\pi}{10}$ with the implementation of the second matrix $K$ by pole placement . . . 49
3.27 The response of the system for $\theta_{10} = \frac{\pi}{10}$ . . . 50
3.28 The response of the real system for $\theta_{10} = \frac{\pi}{10}$ with the implementation of matrix $K$ for $Q = 1$ . . . 51
3.29 The response of the real system for $\theta_{10} = \frac{\pi}{10}$ with the implementation of matrix $K$ for $Q = 10^3$ . . . 51
3.30 The value of $u$ for the real system for $\theta_{10} = \frac{\pi}{10}$ with the implementation of matrix $K$ for $Q = 10^3$ . . . 52
3.31 The value of $u$ for the real system for $\theta_{10} = \frac{\pi}{3}$ with the implementation of matrix $K$ for $Q = 10^3$ . . . 53
3.32 The response of the real system for $\theta_{10} = \frac{\pi}{3}$ with the implementation of matrix $K$ for $Q = 10^3$ . . . 53
3.33 The value of $u$ for the real system for $\theta_{10} = \frac{\pi}{3}$ with the implementation of matrix $K$ for $Q = 10^3$ and saturation . . . 55
3.34 The response of the real system for $\theta_{10} = \frac{\pi}{3}$ with the implementation of matrix $K$ for $Q = 10^3$ and saturation . . . 55
3.35 The response of the real system for $\theta_{10} = \frac{\pi}{3}$ with the previous control system and an integrator (gain 1) . . . 56
3.36 The response of the real system for $\theta_{10} = \frac{\pi}{3}$ with the previous control system and an integrator (gain 30) . . . 56
3.37 The Simulink configuration of the final control scheme for the moving axes case . . . 57

*Dedicated to my parents that have always been there for me*

# Chapter 1

# Introduction

One of the main goals for the field of robotics, and technology in general, has always been the idea of optimizing any action to be performed. In many situations there is a constant search to find the fastest way, or the cheapest or, more often, the most efficient one.

When the need is to move on the ground, for instance, the most common solution is to adopt wheels, varying in number based on the required application. A perfect example for this concept is the more and more common Self-balancing scooter, based on the concept of a Self-balancing robot.

This movement apparatus, however, presents several limitations, one of which concerns the fact that an instantaneous movement is possible only in the direction to which the wheels are pointing. Think for example when people need to parallel park a car: if the car were able to instantly move in any direction, the procedure would be extremely easy since it is only needed to fit inside the space. Instead, due to the working principle of wheels, the driver needs to perform several maneuvers in order to align the wheels in the right directions to fit in the spot.

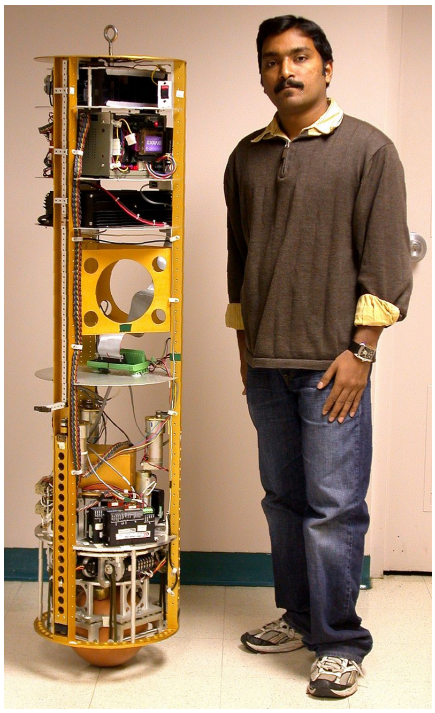

FIGURE 1.1: The first Ball-Balancing Robot built at Carnegie Mellon University, USA in 2005

It was mainly to cope with this kind of limitations that, in 2005, the first Ball-Balancing Robot (or Ballbot) was created. The idea is that, since the body is placed on a sphere instead of a series of cylinders, it is possible for the robot to instantaneously move in any direction, exploiting the polar symmetry of the ball. This working principle has great potential in terms of speed and efficiency of movement since, for example, to change direction the system does not have to waste time and energy to turn the wheels. In fact, thanks to the combined action of the three (or more) motors, it is possible to generate a resultant torque in any direction, without having to change the configuration of the body.

Based on this moving principle, many complex robots can be built with an increased agility and maneuverability with respect to their "standard colleagues".

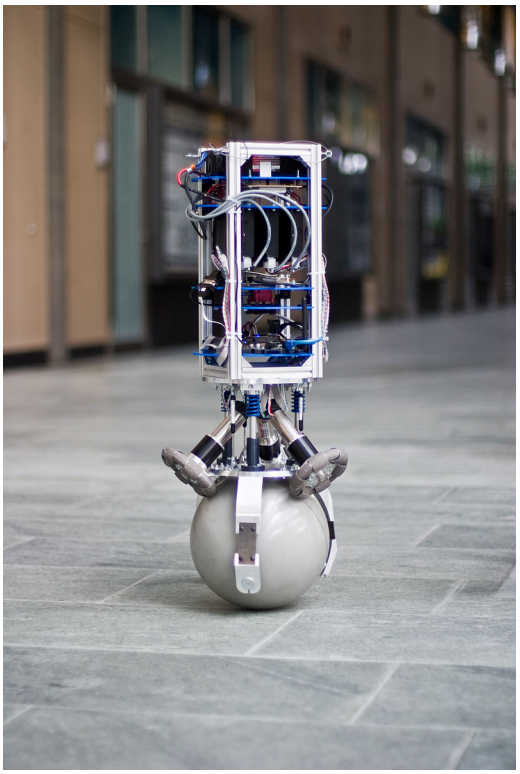

FIGURE 1.2: A later version of ball-Balancing Robot built at ETH Zurich, Switzerland in 2010

This concept was also embraced by the well known cinematic saga of Star Wars. In fact, with the new trilogy that came out a few years ago, the design of the beloved R2-D2 was substituted by the more modern BB-8, that is indeed an advanced form of Ball-balancing Robot! It is not a case that it soon became the inspiration for the realization of this thesis.

FIGURE 1.3: Droid BB-8, from the Star Wars cinematic universe

Since the realization of a real Ballbot is quite a difficult and complex process that greatly surpasses the competencies required for a bachelor degree, this thesis will try to analyse the working principle of this robot from a 2-D point of view.

In particular, instead of considering three wheels acting on a sphere, the study will be simplified towards a case of a wheel acting on a cylinder, that therefore basically represents two generic sections of two cylinders in contact. This allows for a thorough analysis of the concept of coupling due to friction and its behaviour, that can then be combined and rearranged to go back to the 3-D case.

The work will be divided into two main parts: the modelling of the system and its control.

The modelling part will be then split into two sections. The first section deals mostly with the coupling dynamics between the two bodies, considering how the friction affects the transmission of motion from the wheel to the cylinder. It is interesting to notice that the analyzed behaviour can be seen in everyday life with, for example, tyres on a street or train wheels on a rail. The reason is that these two cases can be seen as two cylinders moving on each others with the second one (the ground) having an infinite radius. Therefore, this modelling analysis can be relevant in a wider set of case scenarios.

The second part, instead, also introduces the variables depending on the configuration of the system: if, for example, the top cylinder starts falling due to gravity, what happens to the dynamics of the the bodies?

The control part will basically follow the modelling. This means that there will be a first part where the relative position of the two bodies is not taken into account and is assumed to be fixed. In this case the attention will be towards the necessary input torque that a motor has to generate on the wheel in order to move the body to a specific position.

The second part, instead, deals mostly with stability since, as it is easy to imagine, the real system will be highly unstable and therefore a stabilizing control system needs to be implemented.

Finally, some possible ways to expand this project in the future will be suggested in order to facilitate future studies on the matter.

# Chapter 2

# Modelling

## 2.1 Introduction

In order to fully comprehend the behaviour of the robot, it is necessary to analyze the physical relationship between the wheels of the machine and the cylinder below them.

The system can be simplified as two cylinders in relative motion, where a torque is applied externally to one body and is then transmitted to the second one by means of the physical coupling. It will be clear later that this coupling is due to the friction force between the two bodies.

Notice that, since the analysis is done in 2-D, only a plane section of the cylinders will be considered. For this reason, in the rest of the paper both the words 'cylinders' and 'wheels' will always be referred to these two bodies that will be graphically represented by their section.

For a first analysis, a situation where there is no relative translation of the center of the two cylinders will be considered. In other words, the rotation axis of the two bodies (passing through their centers of mass) will be fixed in space and the contact will be made by means of a fixed force pushing one cylinder towards the other. This allows an initial study of the phenomenon independent from a possible variation of the normal force acting on the two bodies. This first part can be considered as if performed in space, where no external bodies or forces interact with the system, a part from those clearly specified (normal force, load,...).

Then, a condition where the two cylinders are positioned one above the other will be considered. In this case the maximum normal force between the two bodies will correspond to the weight of the cylinder of the top. This value then may decrease depending on the relative position of the two bodies. This introduces a case of variable normal force.

## 2.2 Rolling with fixed rotation axis

As previously said, the idea is to have a first cylinder to which a driving torque is applied. This cylinder is in contact with a second one and it transmits a motion to it by means of a coupling between the two bodies.

This first analysis is done to fully comprehend how the driving torque is transmitted to the second cylinder. In particular the scope of this section is to determine when the rotation between the two bodies is a form of pure rolling or rolling with sliding and the consequent transmission of motion.

For this matter it is useful to first specify the role of dry friction in the linear motion of two objects in contact.

### 2.2.1 Linear analysis of dry friction

Even though in this work two round objects (cylinders) are taken into account, by ideally extending their radius to infinite, two planes are thus obtained. For this reason, this analysis is still relevant towards the modelling of the considered system, with the advantage of being much more intuitive. In particular, some basic notations of physics [9] will be recalled in order to describe the effect of friction on bodies in linear motion.

To explain this simple concept, a box moving on a plane will be considered.

Considering the box initially at rest,it is known that, as soon as an external horizontal force $F_a$ is applied to it, there will be another force $F_{sf}$, exerted on the box by the floor, equal in magnitude and opposite to $F_a$. This tangential force is called static friction force and only appears between two bodies in contact with no relative motion when a tangential force is applied on one of the bodies. As stated before, the magnitude of this friction force $F_{sf}$ will always be equal to that of the applied force $F_a$ up to a limit value given by the expression $F_{sf} \leq \mu_s N$, where $\mu_s$ is a coefficient specific for the two surfaces in contact and $N$ is the normal force acting between the two bodies. As long as the applied force is lower than the limit value of the static friction force, the resultant tangential force on the box will be zero, meaning that no acceleration occurs and the body remains at rest. If instead $F_a$ is grater than the limit value of $F_{sf}$, there will be an acceleration and, consequently, a relative motion between the two surfaces: the body is not at rest anymore.

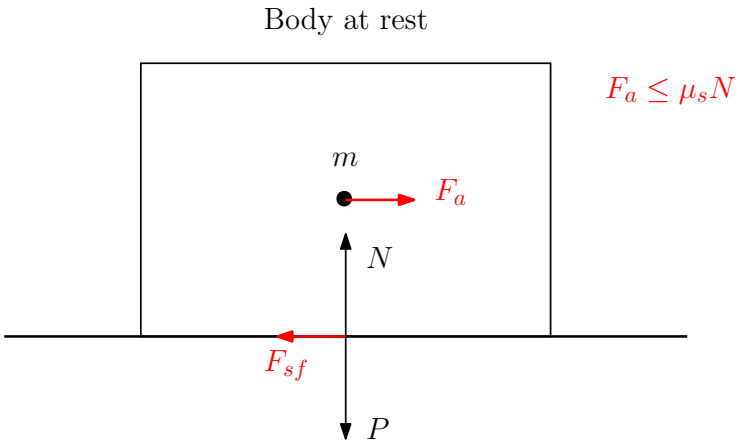


FIGURE 2.1: Linear analysis of static dry friction

In the case of relative motion between the two bodies, static friction is replaced by another form of friction force called dynamic (or kinetic) friction. This force once again opposes the motion of the bodies, but, differently from the static friction one, is always present as long as there is relative speed between the two surfaces, even if no other external tangential force is applied. Moreover, the magnitude of this force has a fixed value corresponding to $F_{df} = \mu_d N$ where $\mu_d$ is once again a coefficient depending on the two surfaces: considering the same two surfaces, its value will always be lower than $\mu_s$. If no other external tangential force is applied to the object, the action of this force will eventually put the system back at rest after a finite period of time.

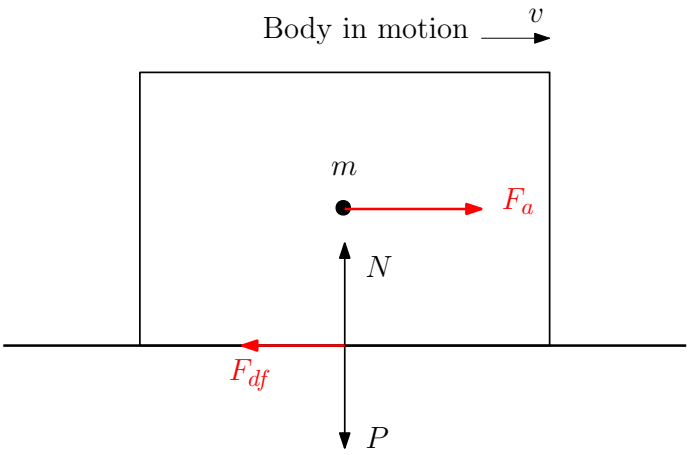


FIGURE 2.2: Linear analysis of dynamic dry friction

With this brief analysis of the subject, it was possible to see that the force applied from the floor to the box is a matter of friction, and the actual magnitude of this force only depends on the physical characteristics of the system ($\mu_s$ and $\mu_d$), on the normal force (in this case the weight of the box was assumed as normal force) and the presence and magnitude of an external tangential force.

The reason, however, for which this section is relevant to the topic of this project is the fact that, due to Newton's third law of motion, the box will exert on the floor a force equal and opposite to the friction force applied from the floor on the box. This fact usually has no importance as the floor is considered a fixed object. However, as soon as we translate this reasoning to the case of two cylinders where both bodies are able to rotate, this phenomenon becomes of utter relevance: the friction force between the two surfaces is the entity that generates the torque on the second cylinder and allows a coupling of the two bodies.

Therefore, it is now necessary to apply this concept to the case of the two cylinders.

### 2.2.2 Rolling behaviour

In the case of rolling of two cylinders, the considerations made before can be applied by converting the concepts from a linear to a rotational environment.

First of all, it is important to understand that the significant factor determining the behaviour of the system is the relative translation of the points of contact of the two bodies. For this reason, in the previous case, no relative motion of the surfaces resulted in the system being at rest. In the rolling case instead, the points of contact of the two bodies can have zero relative speed even if the two cylinders are rotating: the reason is that the points of contact keep changing in time (due to the rotation), but instantaneously there is no translation between them. This case is what is called pure rolling. If instead the point of contact of the two bodies were to instantaneously translate while also continuously changing due to rolling (similarly to what happens when a car drifts), then rolling with sliding occurs.

Considering the concepts introduced before it is now easy to determine the effects of the driving torque in the interaction between the two wheels. The driving torque will generate a transmission force $F_t$ applied from the first to the second cylinder. If this force is lower than the maximum of the static friction force $F_{sf}$, there will be pure rolling, if instead $F_t > F_{sf}$, the force actually transmitted will be capped at

the value given by the dynamic friction force $F_{df}$ and there will be a sliding component in the motion.

This shows that applying an exceedingly high torque would result in a worse transmission of motion as $F_{df}$ is significantly lower than the potential values of transmitted force achievable with pure rolling. In order to return to the condition of ideal coupling given by the pure rolling, it is necessary to reduce the applied torque so that the first cylinder can decelerate enough for the second cylinder to catch up with its pace returning the relative speed back to zero.

### 2.2.3 Rolling friction

Another form of friction will be considered in the study of this dynamic: the rolling friction $C_{rf}$. This phenomenon is caused by the little deformations of the cylinders in the area of contact: the contact surface has a finite area depending on the deformability of the materials. This causes, in case of motion, the force acting on this area to be unevenly spread across the surface due to the motion of the two cylinders: the normal force $N$, in fact, does not act directly on the center of the body, but is slightly shifted towards the direction of motion. The non-uniformity of this force creates a small torque inside the body that counters the moving torque.

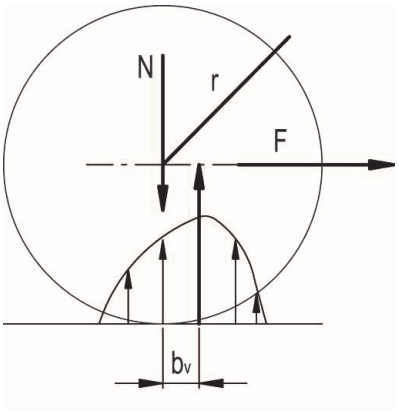


FIGURE 2.3: Diagram showing the principle behind rolling friction

As said, this phenomenon occurs only when there is a rotating motion of a cylinder, meaning that if the system is at rest, this torque is not present. Its maximum magnitude is $C_{rf} = \mu_r N$ where $\mu_r$ is the rolling friction coefficient.

Like dry friction, rolling friction directly counters the motion of the body. For this reason, when the system is at rest, for small applied torques the magnitude of rolling friction directly matches that of the applied torque, making null the resultant of the torques applied to the body and therefore keeping the system at rest. When the applied torque becomes greater than the maximum value of rolling friction torque $C_{rf} = \mu_r N$, rolling friction saturates and the resultant of the torques becomes non null, accelerating the system and putting it in motion. As long as the system keeps being in motion the value of rolling friction will remain capped at it maximum value until the bodies go back to being at rest.

The result of this behaviour on the dynamics of the system differs depending on the situation itself. If the condition for pure rolling is fulfilled ($F_t \leq F_{sf}$) and the system is at rest, then the two cylinders will start moving only when the rolling frictions $C_{rf_1}$ and $C_{rf_2}$ on the two bodies are both overcome by the respective moving torques: in a pure rolling motion the whole system will start moving at the same time

due to the two cylinders being strictly coupled. If instead the system was already in motion with pure rolling, the bodies will accelerate or decelerate depending whether the applied torques $C_1$ and $C_2$ are greater or smaller than the rolling friction torques $C_{rf_1}$ and $C_{rf_2}$.

If instead $F_t > F_{sf}$, sliding is concerned and the two cylinders are not strictly connected anymore: both bodies will accelerate when their own rolling friction is overcome. This means that, if the applied driving torque $C_1$ is smaller than $C_{rf_1}$, the system will be at rest or decelerate. If instead, $C_1 > C_{rf_1}$, but the transmitted torque $C_2$ on the second cylinder is smaller than $C_{rf_2}$, then only the second body will be at rest (decelerate).

### 2.2.4 Conditions recap

Defining as $v_r$ the relative speed of the points of contact of the two cylinders, it is now possible to categorize all the interactions of the two bodies based on the conditions of the system:

| | | |
|---|---|---|
| $v_r = 0$ | $C_1 \leq C_{rf_1}$ OR $C_2 \leq C_{rf_2}$ | $\Rightarrow$ Rest/Deceleration |
| $v_r = 0$ | $C_1 > C_{rf_1}$ AND $C_2 > C_{rf_2}$ | $\Rightarrow$ Pure rolling |
| $v_r \neq 0$ | $C_1 \leq C_{rf_1}$ | $\Rightarrow$ Rest/Deceleration with sliding |
| $v_r \neq 0$ | $C_1 > C_{rf_1}$ AND $C_2 > C_{rf_2}$ | $\Rightarrow$ Rolling with sliding |

The 'Rest/Deceleration' condition depends on the state of the system: in the first case rolling friction only prevents motion, in the second case it decreases the angular speed of the cylinders (much like the relation between static and dynamic friction for linear motions).

It is also significant to remember that the passage from $v_r = 0$ to $v_r \neq 0$, if no other external forces are involved, happens when $F_t > F_{sf}$.

### 2.2.5 Dynamical model with fixed axes

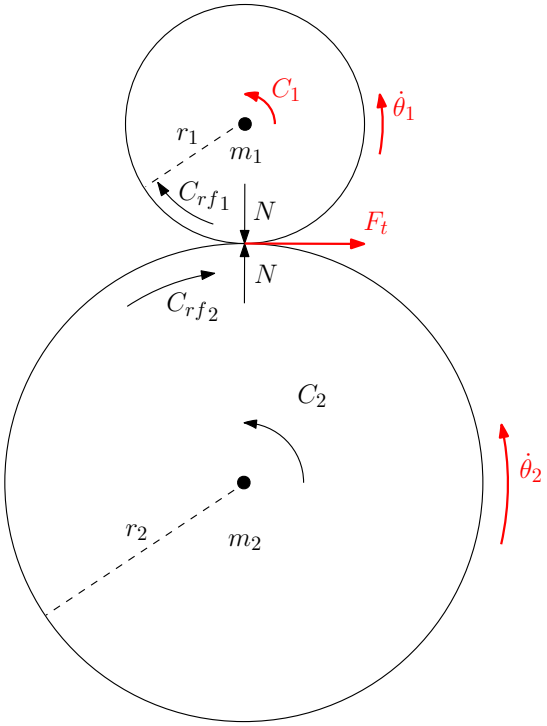


FIGURE 2.4: A 2D overview of the considered system

After all these considerations, it is now possible to define the calculations for the two possible situations.

First of all, using Newton's second law of motion, it is possible to describe the behaviour of the two cylinders in terms of torques applied to them.

The first cylinder will be accelerated by the input driving torque $C_1$ and will be decelerated by the rolling friction torque $C_{rf_1}$. The resultant torque will then "split", as a part of it will have to move the first cylinder (moment of inertia $J_1$), while the other part will have to move the second cylinder (moment of inertia $J_2$) as transmission force $F_t$.

The second cylinder, instead, will be accelerated by the force $F_t$ transmitted from the driving cylinder and will be decelerated by its rolling friction $C_{rf_2}$.

The final equations [1] will, therefore, be:

$$\begin{cases} J_1\ddot{\theta}_1 = C_1 + C_{rf_1} - F_t r_1 \\ J_2\ddot{\theta}_2 = -F_t r_2 + C_{rf_2} \end{cases} \tag{2.1}$$

where the signs are only a matter of notation (note that by definition $C_{rf}$ always has sign opposite to the speed of the body, so it was summed in this expressions).

It is easy to see that, knowing the physical parameters of the system ($r_1$, $r_2$, $m_1$, $m_2$, $\mu_s$, $\mu_d$, $\mu_r$) and the driving torque $C_1$, the only unknowns of the system are the two angular accelerations ($\ddot{\theta}_1$ and $\ddot{\theta}_2$) and the transmission force $F_t$. Obviously, by knowing these three quantities it would be possible to fully define the angular speed of the two bodies and the transmitted torque $C_2$ to the second cylinder.

As was previously stated, however, depending on the conditions related to the driving torque $C_1$, the system will behave in different manners, influencing the value

of $F_t$. It is therefore necessary to define mathematically these conditions and find the corresponding expressions for $F_t$.

First the condition that was expressed as $v_r = 0$ can be clarified. In fact, from a practical point of view, this situation occurs when there is no relative motion at the contact point, that is:

$$v_1 = -v_2 \tag{2.2}$$

where $v_1$ and $v_2$ are the linear speeds respectively of the first and the second cylinder. The negative sign in front of $v_2$ is only a matter of coherence in the notation.

After defining the condition triggering the sliding situation, it is convenient to find the expression of $F_t$ by separating the case of pure rolling to the case where a sliding component is present.

In general the relation between linear and angular speed of a wheel is:

$$v = \dot{\theta} r \tag{2.3}$$

Therefore, in case of pure rolling, it is possible to rewrite Equation (2.2) as a relation linking the two angular speeds $\dot{\theta}_1$ and $\dot{\theta}_2$ as a function of the radii $r_1$ and $r_2$ of the two cylinders:

$$\dot{\theta}_1 r_1 = -\dot{\theta}_2 r_2 \implies \dot{\theta}_2 = -\frac{r_1}{r_2}\dot{\theta}_1 \tag{2.4}$$

Now, adding Equation (2.4) to System (2.1), it is possible to find the expression of the transmission force $F_t$ solving the three-equations system in the three unknowns:

$$F_t = \frac{C_1 J_2 r_1 + C_{rf_1} J_2 r_1 + C_{rf_2} J_1 r_2}{J_2 {r_1}^2 + J_1 {r_2}^2} \tag{2.5}$$

It is interesting to notice that the expression of the force transmitted from the first to the second cylinder depends on both $C_{rf_1}$ and $C_{rf_2}$. The reason for this is due to the fact that the pure rolling condition $\dot{\theta}_2 = -\frac{r_1}{r_2}\dot{\theta}_1$ must be verified. In fact, the presence of $C_{rf_1}$ reduces the available resultant torque on the first cylinder, meaning that there is less available force to be transmitted to the second cylinder as $F_t$. On the other hand, the presence of $C_{rf_2}$ makes it more difficult to move the second cylinder that, therefore, needs a greater force $F_t$ in order to be kept at the same speed of the driving cylinder (in order to fulfill the pure rolling condition). So, in conclusion, $C_{rf_1}$ reduces the available $F_t$, while $C_{rf_2}$ increases the required $F_t$. The balancing of these two factors determines the exact quantity of force to be transmitted in order to keep the system in a pure rolling condition.

For the case of rolling with sliding, instead, the solution is actually much easier to find. In fact, as previously stated, when sliding occurs, the only force transmitted from one body to the other is that of dynamic friction $F_{df}$. Therefore:

$$F_t = F_{df} = \mu_d N \tag{2.6}$$

In conclusion, the transmitted force $F_t$ can be seen as a sort of piecewise-defined function depending on the value of $v_r$:

$$F_t = \begin{cases} \dfrac{C_1 J_2 r_1 + C_{rf_1} J_2 r_1 + C_{rf_2} J_1 r_2}{J_2 {r_1}^2 + J_1 {r_2}^2} & v_r = 0 \\ F_{df} = \mu_d N & v_r \neq 0 \end{cases} \tag{2.7}$$

Now, by rewriting the two Equations (2.1) it is easy to compute the values of the accelerations $\ddot{\theta}_1$ and $\ddot{\theta}_2$ as:

$$\ddot{\theta}_1 = \frac{C_1 + C_{rf_1} - F_t r_1}{J_1} \tag{2.8}$$

$$\ddot{\theta}_2 = \frac{-F_t r_2 + C_{rf_2}}{J_2} \tag{2.9}$$

where the value of $F_t$ is defined in any instant by Function (2.7).

In order to determine instant by instant whether condition $v_r = 0$ is verified, is only necessary to integrate these two results with respect to time to obtain the behavior of the speeds $\dot{\theta}_1$ and $\dot{\theta}_2$. Then, by comparing them with the relation depicted in Equation (2.4), the fulfillment of the condition can be known and the information can be fed back into the system.

With this definition of the quantities involved it is easy to cover all the possible cases. If, during pure rolling, the condition $F_t > F_{sf}$ is fulfilled, automatically $F_t = F_{df}$ and therefore the two speeds $v_1$ and $v_2$ will fall apart. On the other hand, in a rolling with sliding condition, the integrating factor will automatically take care of the fact that the first wheel needs to decelerate enough for the second one to catch up in order to regain the pure rolling condition.

Finally, in order to compute the total torque $C_2$ transmitted to the second wheel, it is just necessary to multiply the transmitted force $F_t$ by the radius $r_2$ of the second cylinder:

$$C_2 = F_t r_2 \tag{2.10}$$

### 2.2.6 Presence of a load

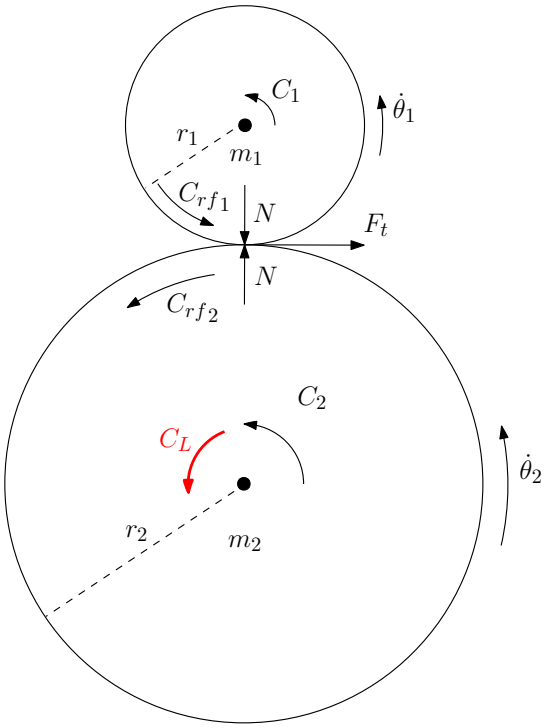


FIGURE 2.5: The system with the addition of the load torque $C_L$

Adding a load torque to the second cylinder does not compromise the functioning of the system.

Calling $C_L$ the load torque, the two Equations (2.1) will become:

$$\begin{cases} J_1\ddot{\theta}_1 = C_1 + C_{rf_1} - F_t r_1 \\ J_2\ddot{\theta}_2 = -F_t r_2 + C_{rf_2} + C_L \end{cases} \tag{2.11}$$

and the expression for the corresponding transmission force $F_t$ will become:

$$F_t = \frac{C_1 J_2 r_1 + C_{rf_1} J_2 r_1 + C_{rf_2} J_1 r_2 + C_L J_1 r_2}{J_2 {r_1}^2 + J_1 {r_2}^2} \tag{2.12}$$

Then $\ddot{\theta}_1$ and $\ddot{\theta}_2$ can be calculated consequently from Equation (2.11).

It is worth underlining that, implementing a torque $C_L$ on the second cylinder variable with respect to the driving torque $C_1$, may cause the angular speeds $\dot{\theta}_1$ and $\dot{\theta}_2$ to change sign during the functioning of the system. This transition causes the contributions of $C_{rf_1}$ and $C_{rf_2}$ to the value of $F_t$ to invert during the motion causing a fast transient in the transmission force that modifies its value according to the physical dimensions of the system.

### 2.2.7 Final equations

Finally, the equations of the system are the following.

$$\begin{cases} \ddot{\theta}_1 = \dfrac{C_1 + C_{rf_1} - F_t r_1}{J_1} \\ \ddot{\theta}_2 = \dfrac{-F_t r_2 + C_{rf_2} + C_L}{J_2} \end{cases} \tag{2.13}$$

With:

$$F_t = \begin{cases} \dfrac{(C_1 + C_{rf_1}) J_2 r_1 + (C_{rf_2} + C_L) J_1 r_2}{J_2 {r_1}^2 + J_1 {r_2}^2} = F_t^\star & v_r = 0 \;\&\; |F_t^\star| \leq \mu_s N \\ F_{df} = \operatorname{sgn}(\dot{\theta}_1 r_1 + \dot{\theta}_2 r_2)\mu_d N & \text{otherwise} \end{cases} \tag{2.14}$$

Consider:

$$C_{rf_1} = -\operatorname{sgn}(\dot{\theta}_1)\mu_r N \tag{2.15}$$

$$C_{rf_2} = -\operatorname{sgn}(\dot{\theta}_2)\mu_r N \tag{2.16}$$

Notice that pure rolling depends both on the condition on relative speed $v_r = 0$ and the one on the static friction force $|F_t^\star| \leq \mu_s N$, which is the passage condition towards sliding.

### 2.2.8 Additional considerations

One last small consideration can be done on the coefficients of friction that were mentioned in this section.

These coefficients were defined as fixed for two particular surfaces. In a real context, though, any small imperfection of the surfaces (wear, presence of external bodies,...) could create a change in the actual value of the coefficients.

For this reason, in order to simulate the behaviour of the system as realistically as possible, a form of small white noise has been applied on the values of these coefficients.

### 2.2.9 Conclusion

In conclusion, in a case of constant normal force applied between the two cylinders, it is possible to compute the angular speeds $\dot{\theta}_1$ and $\dot{\theta}_2$ of those two cylinders as well as the torque $C_2$ transmitted to the second cylinder as long as the physical parameters of the system and the driving torque $C_1$ are known.

## 2.3 Rolling with moving rotation axis

As stated in the introduction, it was first considered a case where the relative position of the rotation axis of the two cylinders could not change. Now, instead, a case with variable rotation axis (but always kept parallel) will be taken into account. In this analysis, the change in the relative position of the axis will result in a change in the direction of normal force between the two cylinders.

The perfect example for this kind of dynamics corresponds to a configuration where the driving cylinder is placed on top of the second cylinder, much like the case of the robot described in this thesis.

Note that, together with the gravity force, also a plane is now influencing the system modifying its behaviour with respect to the previous case. Between the bottom cylinder and the plane a condition of pure rolling will always be assumed.

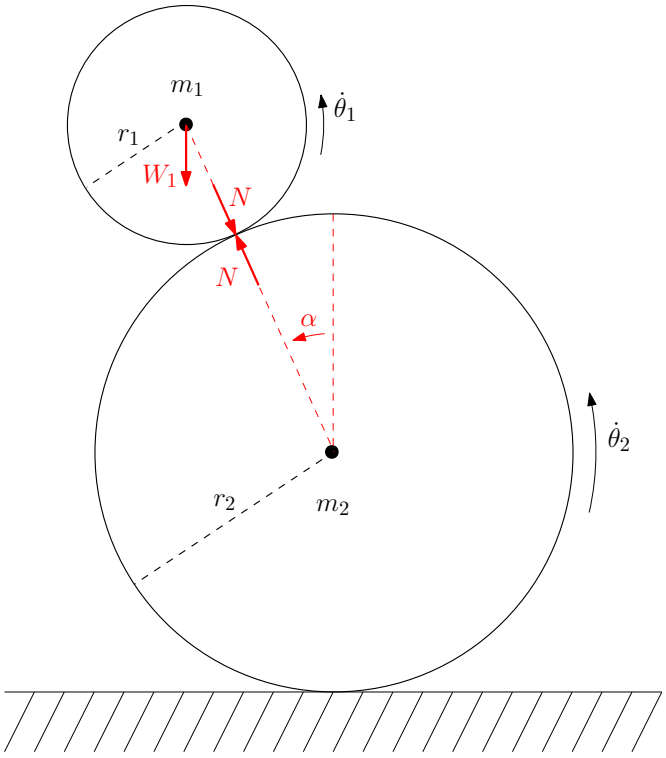


FIGURE 2.6: A 2D overview of the considered system

In this situation, the normal force acting between the two bodies corresponds to the component of the weight of the first cylinder along the line connecting the centers of the faces of the two cylinders.

Obviously the weight $W_1$ of the top cylinder will be calculated taking its mass and multiplying it by the gravitational constant $g$.

$$W_1 = m_1 g \tag{2.17}$$

In order to calculate the component of interest of this force, it is necessary to find the expression of the angle $\alpha$ describing the angular displacement with respect to the vertical of the normal to the point of contact. This angle describes how much the first cylinder has moved on the surface of the second one.

To compute that, it is necessary to consider the fact that the distance considered is an arc of the circumference described by the lower cylinder. It is possible to define this length $a$ of this arc as:

$$a = \alpha r_2 \tag{2.18}$$

### 2.3.1 Change due to relative rotation

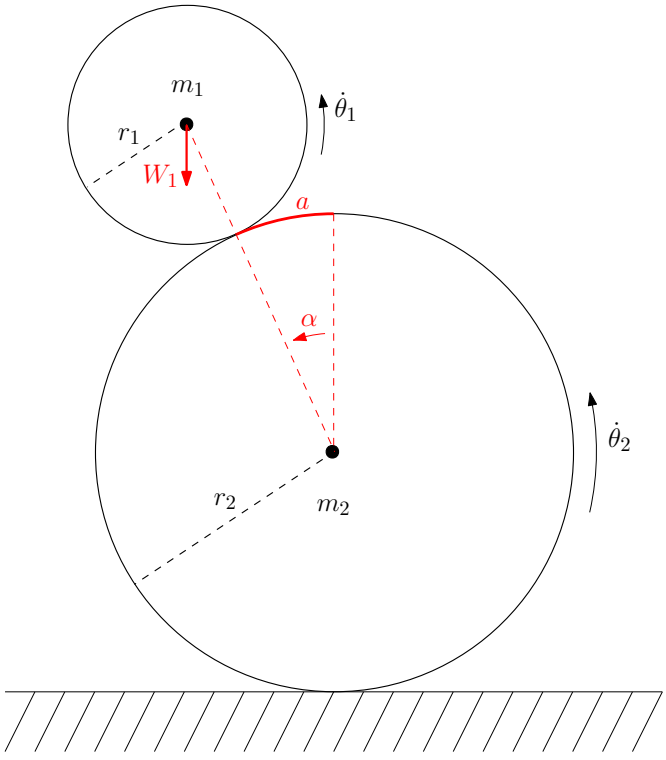


FIGURE 2.7: The geometrical representation of $a$

In this case, the arc described by angle $\alpha$ will be considered as only dependent on the difference between the two arcs described by the movement of the two cylinders.

Calling $a_1$ and $a_2$ respectively these two lengths, $a$ can be defined as:

$$a = a_2 - a_1 = \theta_2 r_2 + \theta_1 r_1 \tag{2.19}$$

where $\theta_1$ and $\theta_2$ are the angular displacements of the two cylinders respectively.

Remember that for the sign convection adopted $\theta_1$ and $\theta_2$ will have opposite signs and therefore the relation is satisfied. By combining Equation (2.18) and Equation (2.19) it is possible to find the expression of $\alpha$ as:

$$\alpha = \theta_1 \frac{r_1}{r_2} + \theta_2 \tag{2.20}$$

This equation, however, proves valid only in a pure rolling situation.

In fact, in a rolling with sliding case the first cylinder will cover an increasingly bigger angle with respect to the second cylinder. However, this extra angle described by the top body does not result in a motion along the surface of the bottom body: the body in fact is sliding.

For this reason, it is necessary to insert a sort of compensation inside the expression of $\alpha$ in order to solve the case of rolling with sliding. Since the rolling with sliding situation coincides with a non null value for the relative linear speed $v_r$. In fact, by integrating the relative speed $v_r$ and deriving the angular value of the displacement by dividing it by $r_2$, it is possible to obtain the compensation value $\frac{d_r}{r_2}$. Therefore, by subtracting this value from Equation (2.20), the expression for $\alpha$ due to relative rotation is obtained:

$$\alpha = \theta_1 \frac{r_1}{r_2} + \theta_2 - \frac{d_r}{r_2} \tag{2.21}$$

The presence of the factor $d_r$ also justifies any initial configuration that could not be obtained with just pure rolling by starting from the standard configuration with $\theta_1 = 0$ and $\theta_2 = 0$. In fact by assigning to $d_r$ the correct value, it is possible to reach any initial configuration.

### 2.3.2 Change due to linear motion

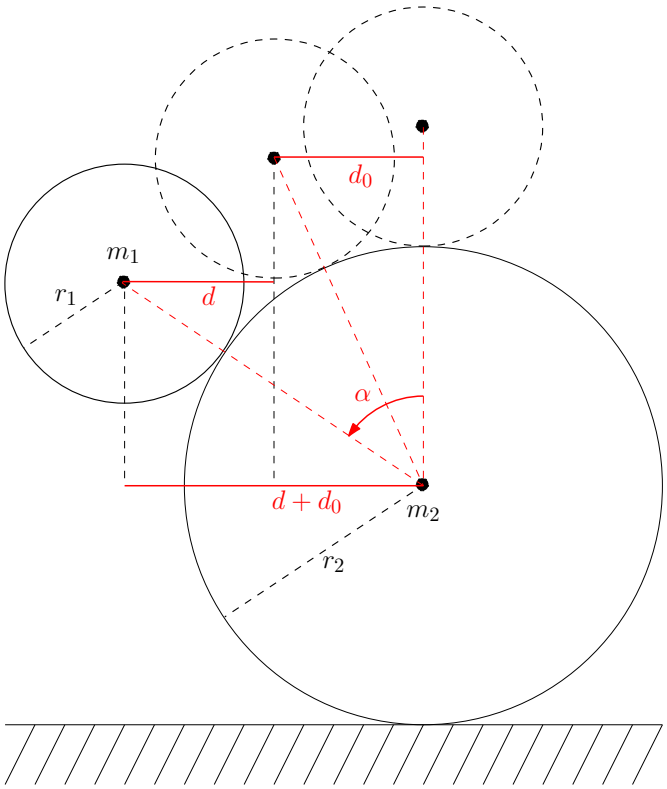


FIGURE 2.8: The geometrical representation of $d$ and $d_0$ as seen from the bottom cylinder

If we now consider the system to be placed on top of a plane, it is easy to understand that the rotation of the second cylinder, as it is in contact with the plane, will cause a linear motion of the body. This phenomenon obviously influences the relative position of the two rotational axis.

If, for the moment, a pure rolling condition between the second cylinder and the plane is considered, the linear displacement $d$ can be computed as:

$$d = -\theta_2 r_2 \tag{2.22}$$

A possible interpretation of the motion is that the top cylinder has no reason to move horizontally and therefore it can be assumed that the horizontal coordinate of its rotational axis will remain still, while that of the second cylinder will change by a quantity $d$.

Moreover, there may be an initial offset on $\alpha$ that influences the system. This possibility will only become relevant in the third chapter, but for completeness it is necessary to account for it in this part. This angular offset can be transformed into a linear offset in order to compare it with $d$. The linear offset $d_0$ caused by $\alpha_0$ on the center of the top cylinder is:

$$d_0 = (r_1 + r_2) \sin(\alpha_0) \tag{2.23}$$

In order to express this behaviour in terms of the angle $\alpha$, by a graphical analysis it can be said that:

$$(r_1 + r_2) \sin(\alpha) = d + d_0 \tag{2.24}$$

and therefore, by substituting Equation (2.22) and Equation (2.23):

$$\alpha = \arcsin\left(\frac{d+d_0}{r_1+r_2}\right) = \arcsin\left(-\theta_2\frac{r_2}{r_1+r_2} + \sin(\alpha_0)\right) \tag{2.25}$$

### 2.3.3 Final $\alpha$ expression

Combining the two dynamics from Equation (2.21) and Equation (2.25), it is possible to write the final expression for $\alpha$:

$$\alpha = \theta_1\frac{r_1}{r_2} + \theta_2 - \frac{d_r}{r_2} + \arcsin\left(-\theta_2\frac{r_2}{r_1+r_2} + \sin(\alpha_0)\right) \tag{2.26}$$

An equivalent analysis could be performed by defining:

$$\alpha = \theta_1\frac{r_1}{r_2} - \theta_2 + \frac{d_r}{r_2} \tag{2.27}$$

However, due to lack of time, this approach will not be considered.

### 2.3.4 Final $N$ calculation

Having now the expression $W_1$ of its maximum value and the angle $\alpha$ describing in any instant its orientation, it is now easy to find the expression for the normal force acting between the two bodies:

$$N = W_1\cos(\alpha) \tag{2.28}$$

where $\alpha$ is the one expressed in Equation (2.26).

### 2.3.5 Tangential component of the weight

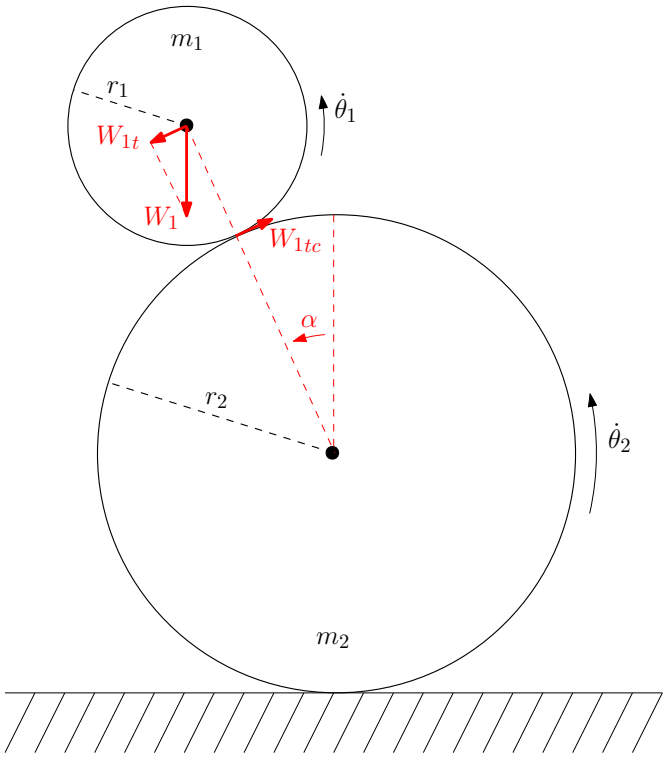


FIGURE 2.9: The geometrical construction to find $W_{1tc}$

Since the contact force between the two cylinders changed direction, it is necessary to take into account the component of the weight force tangential to the contact surface.

Obviously when the top cylinder is perfectly above the lower one this component is null since all the weight force translates into normal force acting directly on the center of mass of the second body. When, however, the top cylinder translates from the vertical position, the tangential component increases thus becoming relevant in the dynamics of the system.

The mathematical expression describing this quantity $W_{1t}$can be easily computed with the angle $\alpha$ previously defined:

$$W_{1t} = W_1 \sin(\alpha) = m_1 g \sin(\alpha) \tag{2.29}$$

It is easy to see that for the vertical position $\alpha = 0$ and therefore $W_{1t} = 0$.

Due to friction between the two cylinders, this force $W_{1t}$ acting tangentially to the contact surface generates a friction force $W_{1tc}$ at the point of contact of the two cylinders and must therefore be taken into account when studying the dynamics of the system.

For the previous case, the condition for which the rolling with sliding behaviour was to be considered was:

$$|F_t| > \mu_s N \tag{2.30}$$

Now, instead, it is necessary to change this formula in order to include the new force. The new condition will then be:

$$|F_t + W_{1tc}| > \mu_s N \tag{2.31}$$

In this way both the forces are taken into account and the system will therefore tend more easily towards a sliding situation.

Also for this new force, when in sliding situation the force it can transmit to the lower body cannot be higher than the dynamic friction force. Therefore:

$$W_{1tc} = \begin{cases} m_1 g \sin(\alpha) & v_r = 0 \\ \text{sgn}(\alpha) F_{df} & v_r \neq 0 \end{cases} \tag{2.32}$$

### 2.3.6 Torque generated by the normal component of the weight

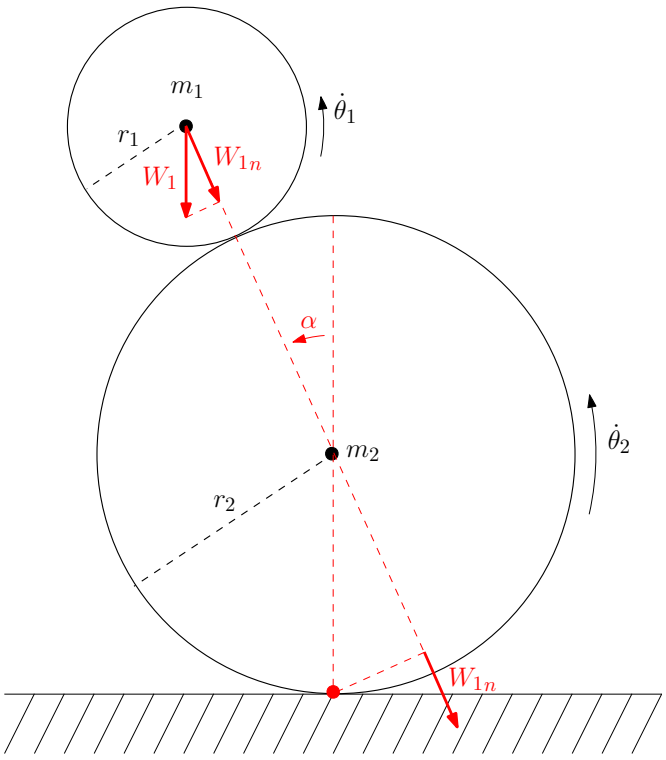


FIGURE 2.10: The geometrical construction to find $C_{W_{1n}}$

Another consideration that has to be made in the case of variable rotation axis is the effect of the normal force in terms of the torque applied on the lower cylinder.

When the system is perfectly vertical, the contact force applied by the top cylinder to the lower one is perfectly balanced by the normal force applied by the ground. However, when the top cylinder shifts from the vertical position, the application point of the normal force is not directly above the contact point with the ground, where the ground normal force is applied. Therefore, the normal component of the weight of the top cylinder is not perfectly balanced by the ground normal force and for this reason generates a torque $C_{W_{1n}}$.

As can be seen from Figure (2.10), this torque is not calculated with respect to the center of mass of the body, but with respect to the center of instantaneous rotation. For this reason, when accounting for this torque, the moment of inertia must take into account Huygens-Steiner theorem:

$$J_{2ir} = J_2 + m_2 {r_2}^2 \tag{2.33}$$

The value of the torque can be calculated as:

$$C_{W_{1_n}} = W_{1n} r_2 \sin(\alpha) \tag{2.34}$$

Now, by combining these two expressions into a dynamic equation, it is possible to show the rotational acceleration generated on the body by this torque:

$$J_{2ir} \ddot{\theta}_2 = -W_{1n} r_2 \sin(\alpha) \tag{2.35}$$

that can be rewritten as:

$$\ddot{\theta}_2 = -\frac{W_{1n} r_2 \sin(\alpha)}{J_2 + m_2 {r_2}^2} \tag{2.36}$$

that is the contribution to the total angular velocity of the second cylinder given by the action of the normal force.

### 2.3.7 Final equations for the system

Taking all these considerations into account, it is now possible to rewrite the final equations for the system by combining the conditions expressed in Equation (2.13) and Equation (2.14) with the expression of $N$ in Equation (2.28) and the two contributions of Equation (2.32) and Equation (2.36). For this case the presence of an arbitrary load $C_L$ will not be considered.
In case of pure rolling, when $\dot{\theta}_1 r_1 = -\dot{\theta}_2 r_2$:

$$\begin{cases} \ddot{\theta}_1 = \dfrac{C_1 - F_t r_1 + C_{rf_1} - W_{1tc} r_1}{J_1} \\ \ddot{\theta}_2 = \dfrac{-F_t r_2 + C_{rf_2} - W_{1tc} r_2}{J_2} - \dfrac{W_{1n} r_2 \sin(\alpha)}{J_2 + m_2 {r_2}^2} \end{cases} \tag{2.37}$$

With :

$$F_t = \begin{cases} F_t^\star & v_r = 0 \ \& \ |F_t^\star + W_{1t}| < \mu_s W_1 \cos(\alpha) \\ F_{df} & otherwise \end{cases} \tag{2.38}$$

$$W_{1tc} = \begin{cases} W_1 \sin(\alpha) & v_r = 0 \\ \operatorname{sgn}(\alpha) F_{df} & v_r \neq 0 \end{cases} \tag{2.39}$$

Where:

$$F_{df} = \operatorname{sgn}(\dot{\theta}_1 r_1 + \dot{\theta}_2 r_2) \mu_d W_1 \cos(\alpha) \tag{2.40}$$

$$F_t^\star = \frac{(C_1 + C_{rf_1} - W_{1tc} r_1) J_2 r_1 + (C_{rf_2} - W_{1tc} r_2) J_1 r_2 - W_{1n} \sin(\alpha) \dfrac{J_1 J_2 {r_2}^2}{J_2 + m_2 {r_2}^2}}{J_2 {r_1}^2 + J_1 {r_2}^2} \tag{2.41}$$

$$C_{rf_1} = -\operatorname{sgn}(\dot{\theta}_1) \mu_r W_1 \cos(\alpha) \tag{2.42}$$

$$C_{rf_2} = -\operatorname{sgn}(\dot{\theta}_2) \mu_r W_1 \cos(\alpha) \tag{2.43}$$

$$W_1 = m_1 g \tag{2.44}$$

$$W_{1n} = W_1 \cos(\alpha) \tag{2.45}$$

$$\alpha = \theta_1 \frac{r_1}{r_2} + \theta_2 - \frac{d_r}{r_2} + \arcsin\left(-\theta_2 \frac{r_2}{r_1 + r_2} + \sin(\alpha_0)\right) \tag{2.46}$$

Taking these results into account, it is easy to understand that the ideal condition for the functioning of the system will be that where the top cylinder is directly on top of the bottom one. The bigger the angular displacement from the vertical axis, the easier will be for the system to shift to a rolling with sliding behaviour and the lower will be the transmitted force in that scenario.

# Chapter 3

# Control

## 3.1 Introduction

Having finished the modelling part, it is now possible to apply the equations found in the former section to try and implement a control of the system.

As for the modelling part, the control analysis will be split in sections with increasing pertinence to the real case. This is done in order to better understand the different steps required for the control.

## 3.2 Control for the fixed axes case

The first and simplest case to be analysed will be the one where we assume the rotation axis of the two cylinders to be fixed in space. To be exact, this time it will be assumed that the cylinders are allowed to translate horizontally, in order to better simulate the case of interest. However, their relative position will never be different from the configuration in which the first cylinders is directly on top of the second one, thus applying a constant normal force.

For this section, the variable to be controlled will only be $\theta_2$: we can assume that the linear translation $d$ of the system will directly depend on this variable as $d = \theta_2 r_2$.

Therefore, the idea behind this section is to find the control system that allows a defined (imaginary) linear translation of the system having $C_1$ as only input, without caring for the relative position of the two rotational axes.

In order to develop the control, a simpler control model will be used. This procedure this the possibility to exploit the condition $v_r \neq 0$, meaning the system will be assumed to always be in pure rolling condition.

### 3.2.1 Transfer function for the fixed axes case

The first necessary step is the one that involves the passage from the dynamics equations to the creation of a suitable transfer function [4].

In order to do so we consider the expressions of $\ddot{\theta}_1$ and $\ddot{\theta}_2$ that were found in Equation (2.13):

$$\ddot{\theta}_1 = \frac{C_1 + C_{rf_1} - \dfrac{(C_1 + C_{rf_1})J_2 r_1 + (C_{rf_2} + C_L)J_1 r_2}{J_2 {r_1}^2 + J_1 {r_2}^2} r_1}{J_1} \tag{3.1}$$

$$\ddot{\theta}_2 = \frac{-\dfrac{(C_1 + C_{rf_1})J_2 r_1 + (C_{rf_2} + C_L)J_1 r_2}{J_2 {r_1}^2 + J_1 {r_2}^2} r_2 + C_{rf_2} + C_L}{J_2} \tag{3.2}$$

That can be rewritten as:

$$\begin{aligned}\ddot{\theta}_1 =& \frac{J_1 {r_2}^2}{J_1 J_2 {r_1}^2 + {J_1}^2 {r_2}^2} C_{rf_1} - \frac{J_1 r_1 r_2}{J_1 J_2 {r_1}^2 + {J_1}^2 {r_2}^2} C_{rf_2} + \\ &+ \frac{J_1 {r_2}^2}{J_1 J_2 {r_1}^2 + {J_1}^2 {r_2}^2} C_1 - \frac{J_1 r_1 r_2}{J_1 J_2 {r_1}^2 + {J_1}^2 {r_2}^2} C_L\end{aligned} \tag{3.3}$$

$$\begin{aligned}\ddot{\theta}_2 =& - \frac{J_2 r_1 r_2}{{J_2}^2 {r_1}^2 + J_1 J_2 {r_2}^2} C_{rf_1} + \frac{J_2 {r_1}^2}{{J_2}^2 {r_1}^2 + J_1 J_2 {r_2}^2} C_{rf_2} - \\ &- \frac{J_2 r_1 r_2}{{J_2}^2 {r_1}^2 + J_1 J_2 {r_2}^2} C_1 + \frac{J_2 {r_1}^2}{{J_2}^2 {r_1}^2 + J_1 J_2 {r_2}^2} C_L\end{aligned} \tag{3.4}$$

As previously mentioned, the output of system will be the position of the center of mass of the lower cylinder. That can be found directly from the angular displacement of the cylinder itself as:

$$d = r_2 \theta_2 \tag{3.5}$$

Now, in order to analyze this system, it is possible to define four states and the input:

$$x_1 = \theta_1 \qquad x_2 = \dot{\theta}_1 \qquad x_3 = \theta_2 \qquad x_4 = \dot{\theta}_2 \qquad u = C_1 \tag{3.6}$$

From here the state-space representation of the system is:

$$\begin{cases} \dot{x}_1 = & x_2 \\ \dot{x}_2 = & \frac{J_1 {r_2}^2}{J_1 J_2 {r_1}^2 + {J_1}^2 {r_2}^2} C_{rf_1} - \frac{J_1 r_1 r_2}{J_1 J_2 {r_1}^2 + {J_1}^2 {r_2}^2} C_{rf_2} + \\ & + \frac{J_1 {r_2}^2}{J_1 J_2 {r_1}^2 + {J_1}^2 {r_2}^2} u - \frac{J_1 r_1 r_2}{J_1 J_2 {r_1}^2 + {J_1}^2 {r_2}^2} C_L \\ \dot{x}_3 = & x_4 \\ \dot{x}_4 = & - \frac{J_2 r_1 r_2}{{J_2}^2 {r_1}^2 + J_1 J_2 {r_2}^2} C_{rf_1} + \frac{J_2 {r_1}^2}{{J_2}^2 {r_1}^2 + J_1 J_2 {r_2}^2} C_{rf_2} - \\ & - \frac{J_2 r_1 r_2}{{J_2}^2 {r_1}^2 + J_1 J_2 {r_2}^2} u + \frac{J_2 {r_1}^2}{{J_2}^2 {r_1}^2 + J_1 J_2 {r_2}^2} C_L \\ y = & r_2 x_3 \end{cases} \tag{3.7}$$

Considering this representation, it is possible to see that the only non-linearity in the equation is represented by the presence of the two rolling friction forces:

$$C_{rf_1} = -\operatorname{sgn}(\dot{\theta}_1) \mu_r N \tag{3.8}$$

$$C_{rf_2} = -\operatorname{sgn}(\dot{\theta}_2) \mu_r N \tag{3.9}$$

For control model purposes, it is possible to treat these two forces as standard dissipative forces in the form $\beta\dot{\theta}$:

$$C_{rf_1} = -\beta \dot{\theta}_1 \tag{3.10}$$

$$C_{rf_2} = -\beta \dot{\theta}_2 \tag{3.11}$$

The system thus becomes:

$$\begin{cases} \dot{x}_1 = & x_2 \\ \dot{x}_2 = & -\dfrac{\beta J_1 {r_2}^2}{J_1 J_2 {r_1}^2 + {J_1}^2 {r_2}^2} x_2 + \dfrac{\beta J_1 r_1 r_2}{J_1 J_2 {r_1}^2 + {J_1}^2 {r_2}^2} x_4 + \\ & + \dfrac{J_1 {r_2}^2}{J_1 J_2 {r_1}^2 + {J_1}^2 {r_2}^2} u - \dfrac{J_1 r_1 r_2}{J_1 J_2 {r_1}^2 + {J_1}^2 {r_2}^2} C_L \\ \dot{x}_3 = & x_4 \\ \dot{x}_4 = & \dfrac{\beta J_2 r_1 r_2}{{J_2}^2 {r_1}^2 + J_1 J_2 {r_2}^2} x_2 - \dfrac{\beta J_2 {r_1}^2}{{J_2}^2 {r_1}^2 + J_1 J_2 {r_2}^2} x_4 - \\ & - \dfrac{J_2 r_1 r_2}{{J_2}^2 {r_1}^2 + J_1 J_2 {r_2}^2} u + \dfrac{J_2 {r_1}^2}{{J_2}^2 {r_1}^2 + J_1 J_2 {r_2}^2} C_L \\ y = & r_2 x_3 \end{cases} \tag{3.12}$$

The state matrices can therefore be defined as:

$$A = \begin{bmatrix} 0 & 1 & 0 & 0 \\ 0 & -\dfrac{\beta J_1 {r_2}^2}{J_1 J_2 {r_1}^2 + {J_1}^2 {r_2}^2} & 0 & \dfrac{\beta J_1 r_1 r_2}{J_1 J_2 {r_1}^2 + {J_1}^2 {r_2}^2} \\ 0 & 0 & 0 & 1 \\ 0 & \dfrac{\beta J_2 r_1 r_2}{{J_2}^2 {r_1}^2 + J_1 J_2 {r_2}^2} & 0 & -\dfrac{\beta J_2 {r_1}^2}{{J_2}^2 {r_1}^2 + J_1 J_2 {r_2}^2} \end{bmatrix} \tag{3.13}$$

$$B = \begin{bmatrix} 0 \\ \dfrac{J_1 {r_2}^2}{J_1 J_2 {r_1}^2 + {J_1}^2 {r_2}^2} \\ 0 \\ -\dfrac{J_2 r_1 r_2}{{J_2}^2 {r_1}^2 + J_1 J_2 {r_2}^2} \end{bmatrix} \tag{3.14}$$

$$C = \begin{bmatrix} 0 & 0 & r_2 & 0 \end{bmatrix} \tag{3.15}$$

$$D = 0 \tag{3.16}$$

From these matrices it is now possible to define the transfer function representing the system using the formula:

$$G(s) = C(sI - A)^{-1} B + D \tag{3.17}$$

In order to find a numerical value for the transfer function of the system it is necessary to assign some arbitrary quantities for the parameters taken into account:

$$m_1 = 5\,kg \tag{3.18}$$
$$m_2 = 20\,kg \tag{3.19}$$
$$r_1 = 0.2\,m \tag{3.20}$$
$$r_2 = 0.5\,m \tag{3.21}$$
$$\beta = 0.0065 \tag{3.22}$$

From which:

$$J_1 = \frac{1}{2} m_1 {r_1}^2 = 0.1\,kg * m^2 \tag{3.23}$$
$$J_2 = \frac{1}{2} m_2 {r_2}^2 = 2.5\,kg * m^2 \tag{3.24}$$

With these values, matrix $A$ becomes:

$$A = \begin{bmatrix} 0 & 1 & 0 & 0 \\ 0 & -0.0130 & 0 & 0.0052 \\ 0 & 0 & 0 & 1 \\ 0 & 0.0052 & 0 & -0.0021 \end{bmatrix} \tag{3.25}$$

whose eigenvalues are $[0, 0, -0.0151, 0]$.

The other matrices are:

$$B = \begin{bmatrix} 0 \\ 2 \\ 0 \\ -0.9615 \end{bmatrix} \tag{3.26}$$

$$C = \begin{bmatrix} 0 & 0 & 0.5 & 0 \end{bmatrix} \tag{3.27}$$

$$D = 0 \tag{3.28}$$

And the final transfer function therefore is:

$$G(s) = -0.4808 \frac{s + 0.0022}{s^2(s + 0.0151)} \tag{3.29}$$

By comparing the eigenvalues of matrix $A$ with the poles of the transfer function it is possible to deduce there has been a pole-zero cancellation in the origin. One possible reason for this cancellation is the fact that, while in pure rolling, $\theta_1$ and $\theta_2$ are strictly related and, therefore, can be described by a single variable. For this reason, only three variables would be required to describe the four states of the system

### 3.2.2 Controller design for the fixed axes case

#### Definition of the specifics

Having defined the transfer function, the next step is the design of a controller [5] that allows the system to respond to a reference signal indicating a position by actually reaching that position.

To do so, the first necessary step is to define certain conditions to be fulfilled. The first condition would be that the system reaches the exact position indicated by the reference: the steady state error must therefore be equal to zero.

On the other hand, a possible dynamic requirement for the system is to keep an overshoot null or as low as possible. This results in the cylinders not going beyond the reference position when moving. For the moment it is instead possible to assume a very permissive requirement regarding the setting time since at this point of the analysis the attention is more turned towards the "quality" of the movement rather than the speed to perform it. For this reason, a settling time of 10 seconds will be just used as a reference, but will represent no real hard condition.

The last, and probably most important, requirement regards the input $u$ to the system: the torque $C_1$ provided by the motor must not overcome the static friction torque thus preventing a rolling with sliding situation. In fact, in order to define the transfer function of the plant, an assumption regarding the pure rolling condition was made and now must be respected to make the control system as coherent as possible for the real case application.

To sum up, the conditions for the system are:

- steady state error equal to zero
- reduced overshoot
- limitation on the input $u$

The first requirement is intrinsically fulfilled by the plant itself since, thanks to the Internal Model Principle, it is known that for a constant reference signal to be perfectly followed (error asymptotically zero)it is sufficient and necessary to have at least one pole in the open loop transfer function $L(s) = R(s)G(s)$. Since the plant, represented by $G(s)$, presents three poles in the origin, this requirement is automatically fulfilled.

The second requirement is, in general, fulfilled with a condition of maximum overshoot smaller than 5%. This condition, from a practical point of view, corresponds to absence of overshoot. As previously said, the condition on settling time below 10s is instead very permissive. From these two conditions it is possible to deduce the dynamic characteristics for the system in the form of characteristics of the open loop transfer function $L(s) = R(s)G(s)$. In particular, the specific on overshoot requires a phase margin $M_f$ that satisfies:

$$M_f^\star \geq 75^\circ \tag{3.30}$$

The specific on settling time, instead indicates a range for crossing pulsation that can be calculated as:

$$\omega_c{}^* \geq \frac{4.6}{0.75 * 10} = 0.61\, rad/s \tag{3.31}$$

### Stabilization of the system with static gain

First thing to do is see whether the uncontrolled system is stable. It is easy to see that the plant $G(s)$ has a negative gain, therefore the controller needs to have a negative gain as well in order to make a total positive gain for the open loop transfer function $L(s)$. For now it is enough to have $R(s) = -1$ by selecting the static gain of the controller: $R(0) = -1$.

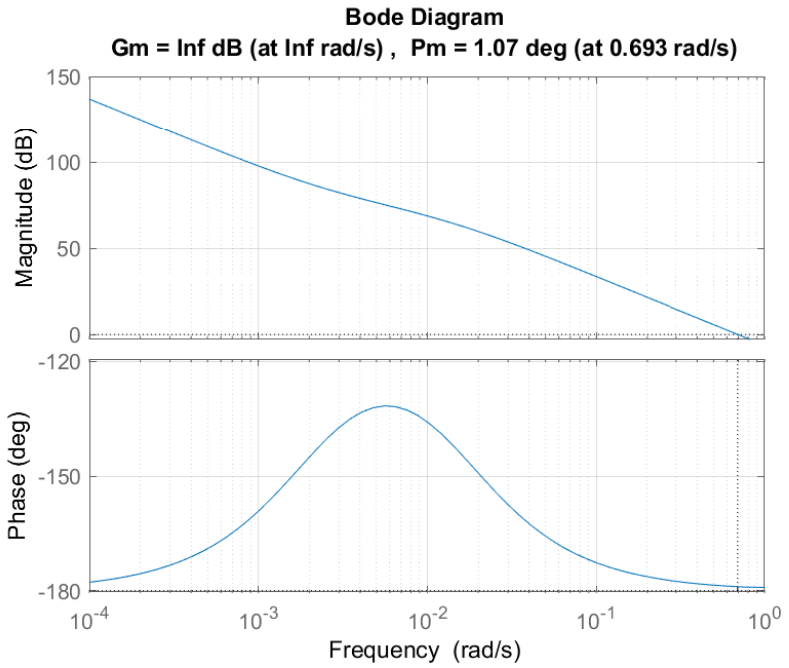


FIGURE 3.1: The bode diagram of the system with only $R(s) = -1$

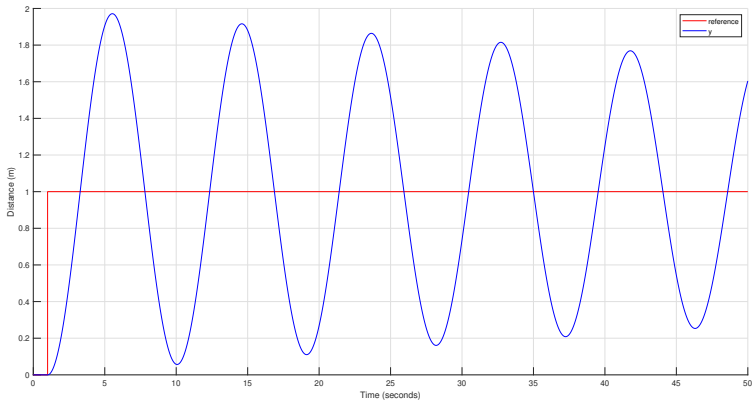


FIGURE 3.2: The step response of the closed loop system with only $R(s) = -1$

Now, by plotting the step response of the closed loop system, it is possible to see that the system is indeed asymptotically stable, but highly oscillating since the phase margin is really small (1.07°). The positive thing, however, is that the crossing pulsation already has an ideal value of 0.693 rad/s: it is within the imposed range without being too high. Remember that an excessively high value would require a high control input, that needs instead to be kept low for this system.

**Implementation of anticipatory networks**

All things considered, a controller able to increase the phase margin at the required crossing pulsation should be enough to deal with this requirement. To do so, the best approach is to use anticipatory control networks: they increase the phase margin at a given pulsation minimizing the effect on the amplitudes. They are characterized by a real zero at lower frequencies compensated by a real pole at higher frequencies. The pole is basically a physical feasibility pole.

It is already possible to understand that in order to generate the wanted increase in the phase margin it will be necessary to use at least two networks: theoretically a single net can compensate for a maximum of 90°, however it would require a great control effort, therefore it is much more efficient to use two nets for required increases in phase grater than 70°. We can assume the two nets to have coincident zeros and poles, in order to facilitate the design.

The first operation would be to define a desired crossing pulsation. In this case it will not be strictly necessary to meet that pulsation in the end, but it is convenient to keep it as a reference. In particular the choice will be:

$$\omega_c{}^* = 0.7\, rad/s \tag{3.32}$$

From here, it is possible to already define the position of the two physical feasibility poles. They must be ideally one decade after the crossing pulsation: if they were closer, their effect would be too big on the amplitudes, if they were farther they would "intervene" later to compensate the zeros resulting in a high control effort for the system. Actually the poles should be defined at the end of the design, however in this project this procedure was preferred since, even if minimal, the poles have an effect on the amplitudes of the function at the crossing pulsation: by taking them into account at the beginning of the design it is possible to compensate them with the position of zeros and the gain.

The parameter for the poles will thus be:

$$\tau_p = \frac{1}{10\omega_c{}^*} = 0.1429 \tag{3.33}$$

And the provisional regulator will therefore be:

$$R(s) = -\frac{1}{(1+\tau_p s)^2} \tag{3.34}$$

By studying the bode plot of the provisional open loop transfer function $L(s) = -\frac{1}{(1+\tau_p s)^2} * G(s)$ it is possible to see that, accounting for the action of the poles, the new positive change in phase must be of 85,2°. Considering there are two zeroes to obtain the wanted change in phase, each zero must do half the work, resulting in a lower effort. For this reason the parameter $\rho$ is defined as:

$$\rho = \tan\left(\frac{85.2}{2}\right) = 0.9195 \tag{3.35}$$

From here, the parameter for the two zeroes is:

$$\tau_z = \frac{\rho}{\omega_c} = 1.3136 \tag{3.36}$$

The provisional regulator therefore is:

$$R(s) = -\frac{(1+\tau_z s)^2}{(1+\tau_p s)^2} \tag{3.37}$$

By studying the bode plot of the new open loop transfer function, though, it is easy to notice that by crossing at 0.7 rad/s, the positive change in phase given by the two zeroes is not fully exploited. If instead the function crosses at 2.3 rad/s the peak of the phase displacement is used, meaning a larger phase margin is obtained by using the same two poles. Since there is no strict requirement regarding the crossing frequency and the overshoot is desired as low as possible, a static gain is added in order to make the function cross at 2.3 rad/s. The static gain expression is:

$$\mu = 10^{\frac{1.61}{20}} = 1.2036 \tag{3.38}$$

So now it is possible to define the whole regulator as:

$$R(s) = -\mu\frac{(1+\tau_z s)^2}{(1+\tau_p s)^2} = -1.2036\frac{(1+1.3136s)^2}{(1+0.1429s)^2} \tag{3.39}$$

Now it is possible to write the final open loop transfer function:

$$L(s) = R(s)G(s) \tag{3.40}$$

And the final complementary sensitivity function:

$$F(s) = \frac{L(s)}{1+L(s)} = \frac{R(s)G(s)}{1+R(s)G(s)} \tag{3.41}$$

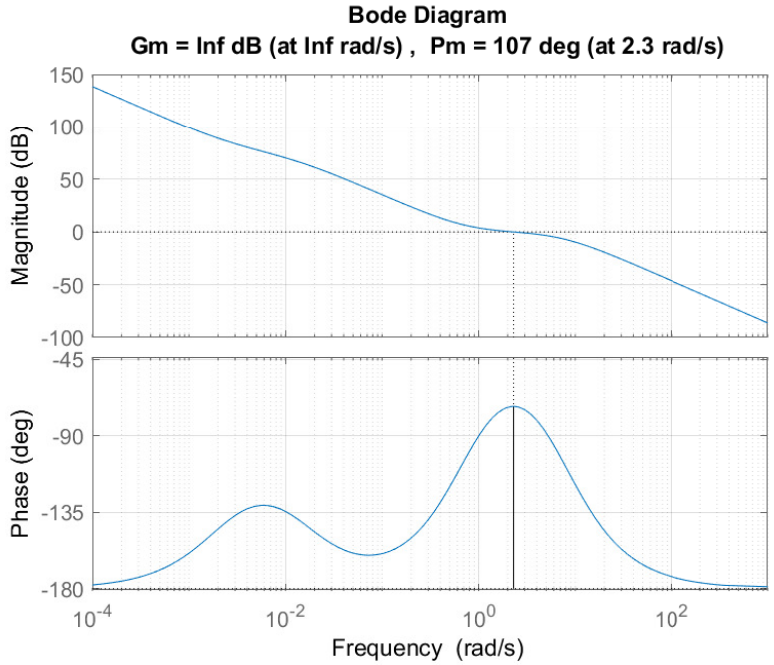


FIGURE 3.3: The bode diagram of L(s)

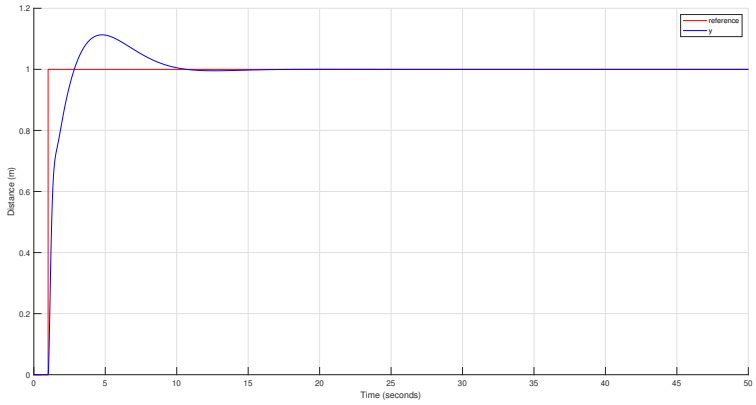


FIGURE 3.4: The step response of F(s)

It is easy to see the overshoot is low, but could be lower, while the settling time is coherent to the reference of 10s that was imposed at the beginning of the design.

The main problem, though, is related to the input variable $u$.

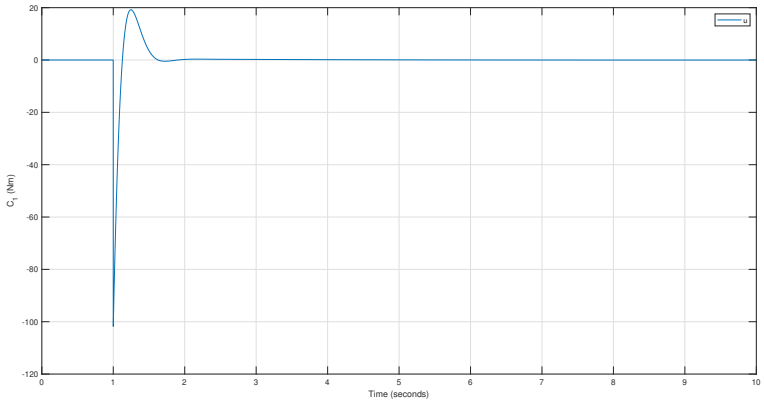


FIGURE 3.5: The value of $u$ in time after a step input of 1

As can be seen from the graph, at the beginning of the transitory the input value reaches very high negative values, while in order to keep a pure rolling condition it is necessary for them to be much lower.

### Implementation of a prefilter

In order to try and reduce as much as possible the overshoot and, most importantly, highly reduce the control input $u$, a solution concerning a prefilter should be introduced.

A prefilter is a low-pass filter that is introduced just after the input and before the control loop. This controller helps reduce the control variable by filtering the frequencies of the input signal higher than the crossing pulsation. By doing so it slightly slows the system, but reduces the overshoot, as will be seen by comparing Figure (3.5) with Figure (3.8)

A suitable prefilter for this project is one of the second order that has the expression:

$$R_{pf}(s) = \frac{1}{(1+\tau_{pf}s)^2} \tag{3.42}$$

With:

$$\tau_{pf} = \frac{0.65}{\omega_c{}^*} = 0.9286 \tag{3.43}$$

By adding the prefilter to the system, the following configuration is obtained:

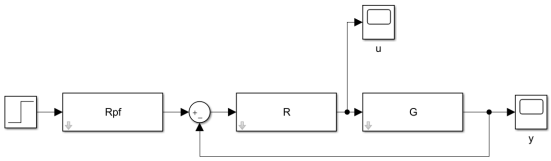


FIGURE 3.6: The Simulink configuration of the system

Thanks to the prefilter the control input u is now reduced to the following values:

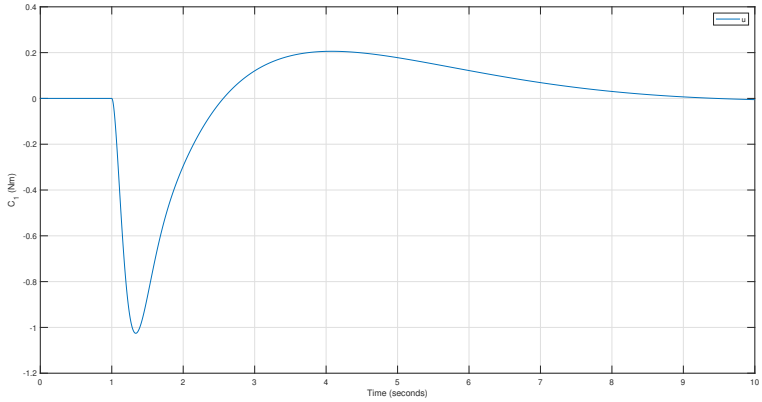


FIGURE 3.7: The values of $u$ in time for the prefiltered system after a step input of 1

These are consistent with the requirements stated at the beginning of the design. Obviously, they depend on the input signal: the higher the input (distance to be covered by the robot), the higher will be the necessary torque to perform the movement in a given time.

Moreover, also the step response of the whole system is slightly improved since the overshoot has been mitigated by the prefilter.

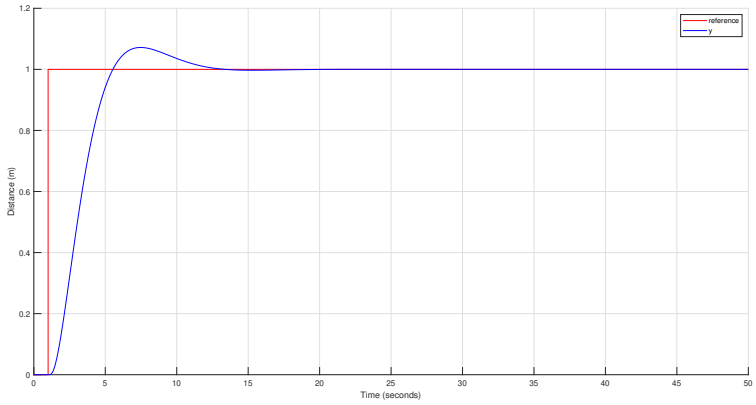


FIGURE 3.8: The step response of the final system

With these considerations the analysis on the control model is finished and the control system now must be tested with the real system.

### 3.2.3 Implementation on real system for the fixed axes case

#### Addition of an integrator

By implementing this control scheme with the real system, it is immediately evident that there is a significantly high error in steady state.

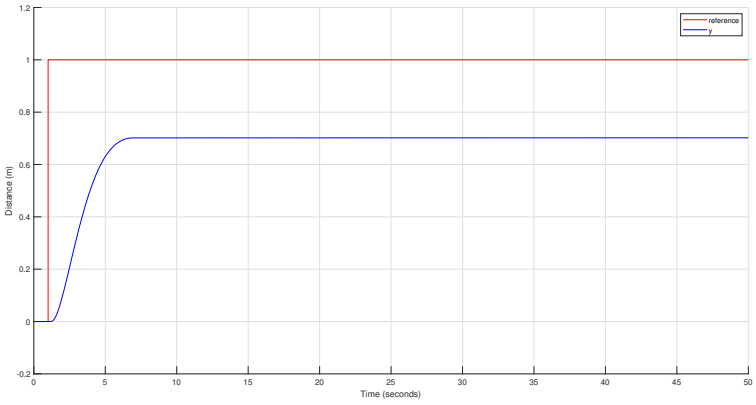


FIGURE 3.9: The step response of the real system with respect to the reference

The reason for this behaviour is that an important assumption was made when dealing with the control model. It was decided that it was not necessary to add an integrator to the regulator since the plant $G(s)$ already had two poles in the origin and would therefore automatically deal with error in steady state.

The real system, however, has a more complex dynamics. It is thus necessary to add an integrator to the controller when dealing with real systems.

The design of the regulator $R(s)$ must be redone with this fact in mind. Due to the presence of a pole in the origin of the regulator, three zeros (and three physical feasibility poles) are now necessary to obtain the wanted phase margin. The rest of

the design procedure is the same as shown before. In the end the final regulator is:

$$R(s) = -\mu \frac{(1+\tau_z s)^3}{s(1+\tau_p s)^3} = -0.1202 \frac{(1+2.5772s)^3}{s(1+0.1429s)^3} \tag{3.44}$$

Now, plotting the step response of the real system with this new regulator the following result is obtained:

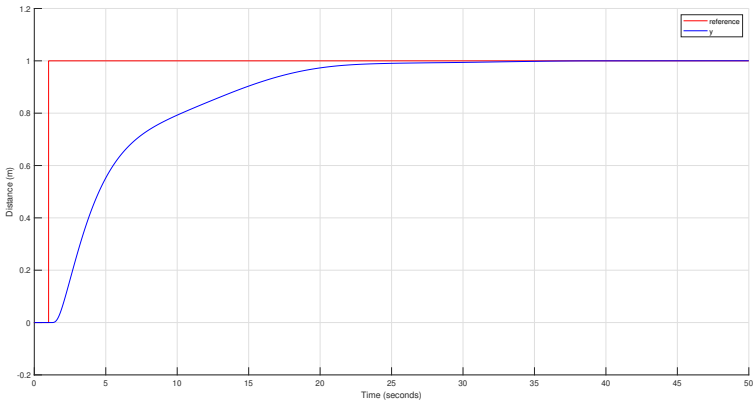


FIGURE 3.10: The step response of the real system with respect to the reference after adding an integrator

This time the signal perfectly follows the reference at steady state.

### Elimination of the settling tail

However, it is easy to see that the response of the system is characterized by a marked settling tail that greatly increases the settling time. The reason for this is given by the fact that the feedback system will have at least a couple of pole and zero that almost cancel out. In order to try and avoid this behaviour, a possible solution is trying to move the zeroes at higher frequencies in order to improve their behaviour.

To do so the regulator is redesigned with a higher crossing frequency due to the higher frequency of the zeroes. The new regulator therefore is:

$$R(s) = -\mu \frac{(1+\tau_z s)^3}{s(1+\tau_p s)^3} = -46.2381 \frac{(1+0.3559s)^3}{s(1+0.0200s)^3} \tag{3.45}$$

With this new regulator the step response of the controlled system is:

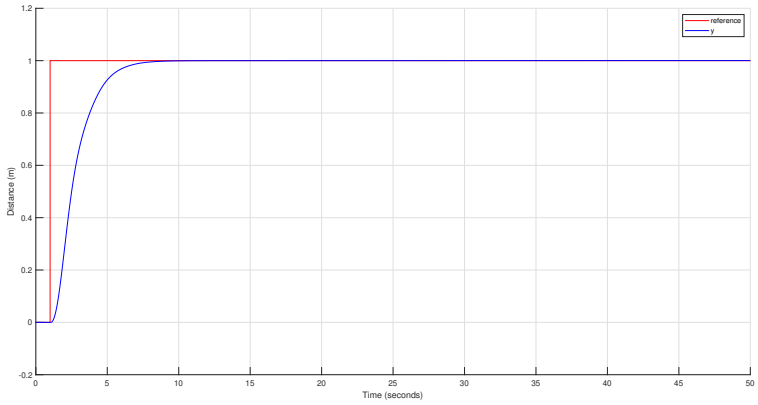


FIGURE 3.11: The final step response of the real system with respect to the reference

Now the system presents zero steady state error, zero overshoot, a settling time below 10s and, most importantly, a reduced control input that prevents the system from sliding.

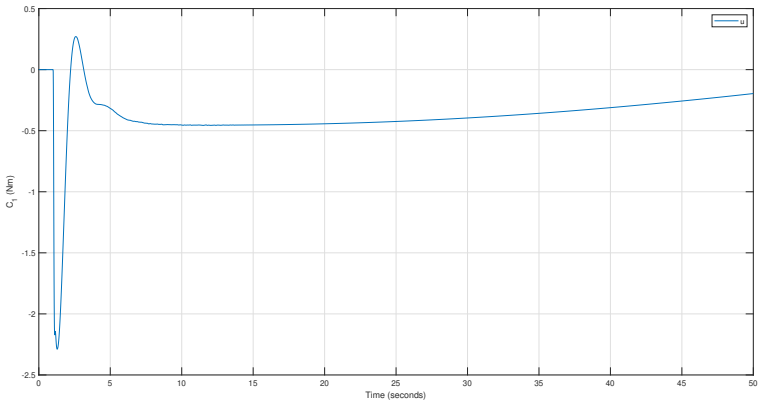


FIGURE 3.12: The final control input to the system with a step reference of 1m

### 3.2.4 Presence of a load

By implementing the previous control scheme on a real system with the addition of a constant load on the lower cylinder, it is possible to see that the controllers work perfectly also in this case, either for a positive or a negative load.

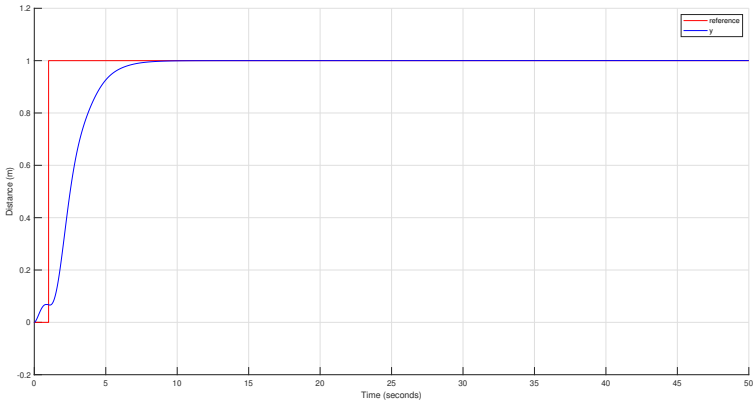


FIGURE 3.13: The step response of the system with a positive load of 10Nm

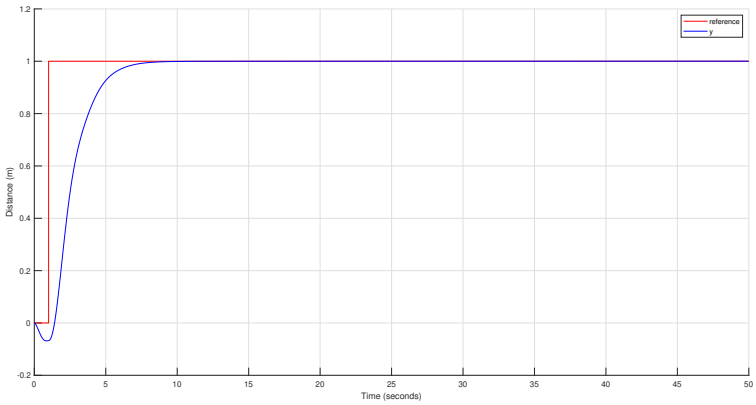


FIGURE 3.14: The step response of the system with a negative load of -10Nm

It is easy to see that the only difference in the step response is an initial movement of the cylinders given by the load before the step reference signal comes in. Note that also the initial movement is managed by the control scheme that tends to reduce the effect of the load on the position of the system.

The main difference in presence of a load is the control input $u$ that needs to be bigger in absolute value in order to deal with the load.

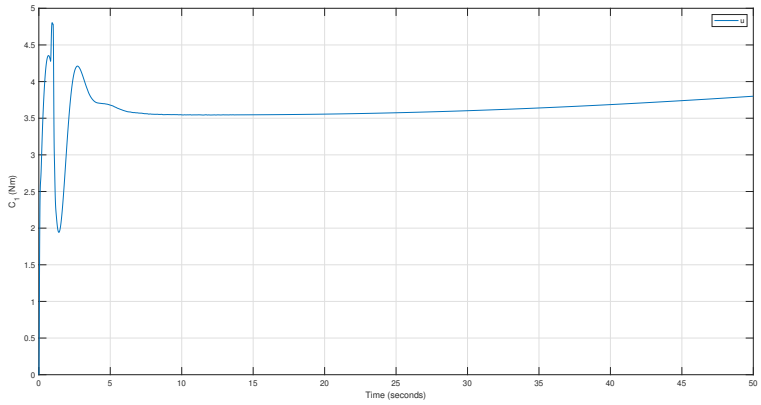


FIGURE 3.15: The control input to the system with a positive load of 10Nm

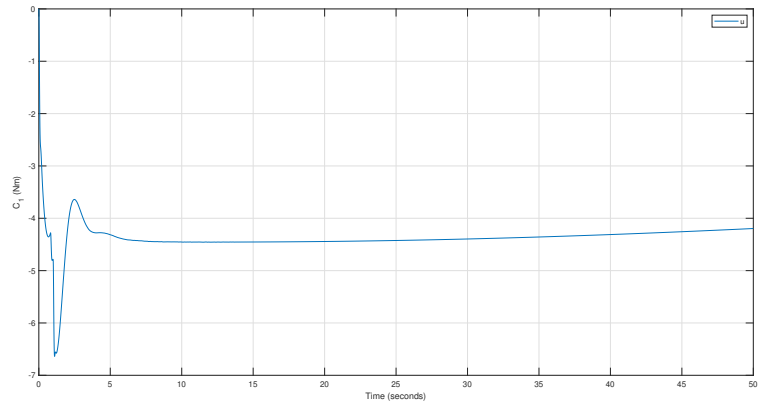


FIGURE 3.16: The control input to the system with a negative load of -10Nm

Therefore, as long as the long as the load and the reference signal are not too big as to require an excessive control input, the controllers are able to manage the system by applying a torque that does not push the system to a rolling with sliding behaviour.

### 3.2.5 Saturation of the control input

#### Definition and application of the saturation

As previously said, the use of a prefilter helps reduce the values of the control input in order to try and keep the system in a pure rolling condition. However, it is necessary to also consider the case where the prefilter is not enough. In those cases, in order for the system to work properly, it is important to avoid sliding, and therefore a saturation on the control input must be introduced. In order to understand which value the input torque must not overcome, the relation on Equation (2.14) must be taken into account. From that relation it is possible to state that the condition for the

system to remain in pure rolling is:

$$|F_t| < \mu_s N \implies \left| \frac{(C_1 + C_{rf_1})J_2 r_1 + (C_{rf_2} + C_L)J_1 r_2}{J_2 {r_1}^2 + J_1 {r_2}^2} \right| < \mu_s N \tag{3.46}$$

Solving this relation for $C_1$ the result is:

$$\begin{cases} C_1 > \dfrac{-\mu_s N(J_2 {r_1}^2 + J_1 {r_2}^2) - (C_{rf_2} + C_L)J_1 r_2}{J_2 r_1} - C_{rf_1} \\ C_1 < \dfrac{\mu_s N(J_2 {r_1}^2 + J_1 {r_2}^2) - (C_{rf_2} + C_L)J_1 r_2}{J_2 r_1} - C_{rf_1} \end{cases} \tag{3.47}$$

Therefore the upper and lower limit for the control input $C_1$ are defined.

Actually, the two values change in time depending on the sign of $C_{rf_1}$ and $C_{rf_2}$. Therefore the best idea is to keep a safety margin for both values and define constant upper and lower bounds $C_{1max}$ and $C_{1min}$. For the arbitrary values assigned, two good values would be:

$$C_{1max} = 7.7\ Nm \tag{3.48}$$

$$C_{1min} = -7.7\ Nm \tag{3.49}$$

By implementing a saturation in the control system it is now possible to deal with higher loads or reference signals of higher value without worrying about the rolling with sliding condition.

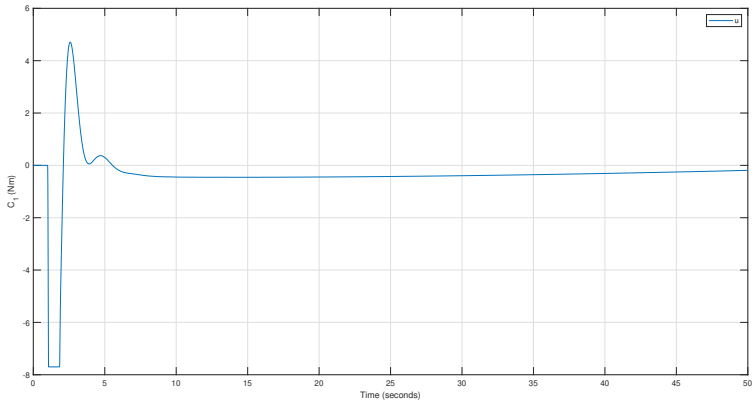


FIGURE 3.17: The control input to the system with a reference of 5m and no load with saturation

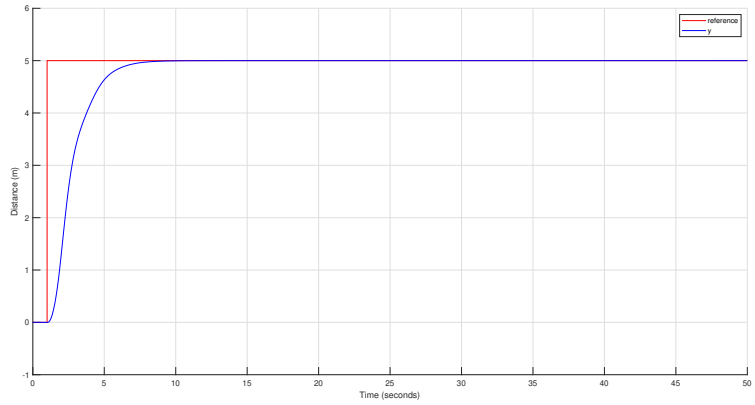


FIGURE 3.18: The step response of the system with a reference of 5m and no load with saturation

As can be seen from Figure (3.17), without the saturation the control input would have overcome the maximum allowed for pure rolling and the system would have therefore started sliding, highly compromising the final response.

In this case the windup behaviour given by the saturation of the integral action in the controller hardly creates any problem.

If, instead, the reference signal is made even bigger, it is possible to see the huge problem given by the windup since the system becomes completely unable to deal with reference signal.

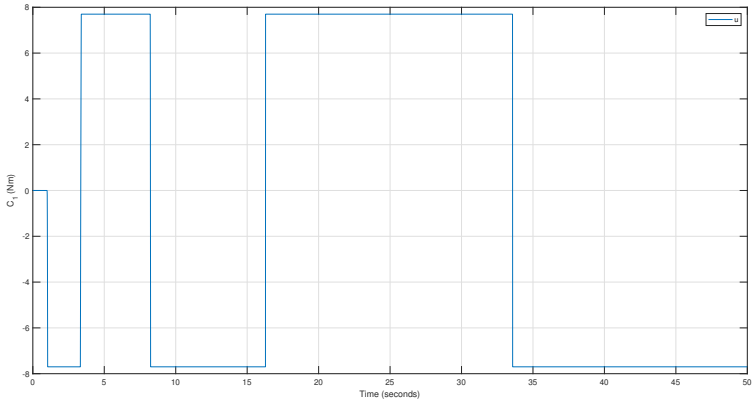


FIGURE 3.19: The control input to the system with a reference of 10m and no load with saturation

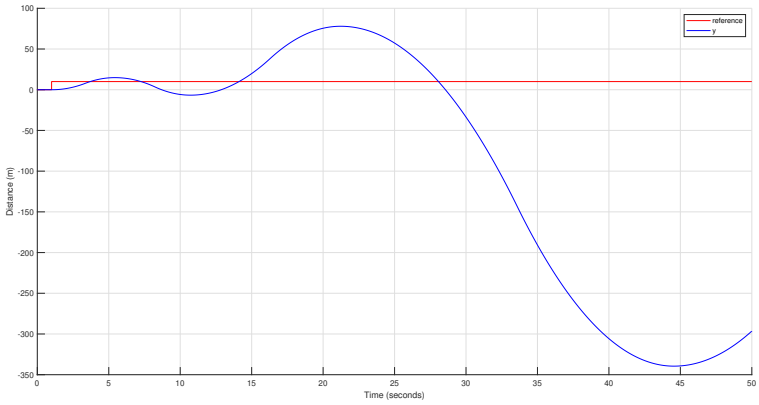


FIGURE 3.20: The step response of the system with a reference of 10m and no load with saturation

**Implementation of an anti-windup network**

In order to deal with this problem, an anti-windup network must be introduced. For its design, the arbitrary polynomial will be:

$$\Gamma(s) = (s+10)^4 \tag{3.50}$$

Therefore, before the saturation there will be a regulator:

$$R_a = -\mu \frac{(1+\tau_z s)^3}{(s+10)^4} \tag{3.51}$$

And in the feedback loop of the saturation there will be:

$$R_b = \frac{(s+10)^4 - s(1+\tau_p s)^3}{(s+10)^4} \tag{3.52}$$

Then, following the control scheme of the anti-windup network making use of the polynomial $\Gamma(s)$, the following results are reached.

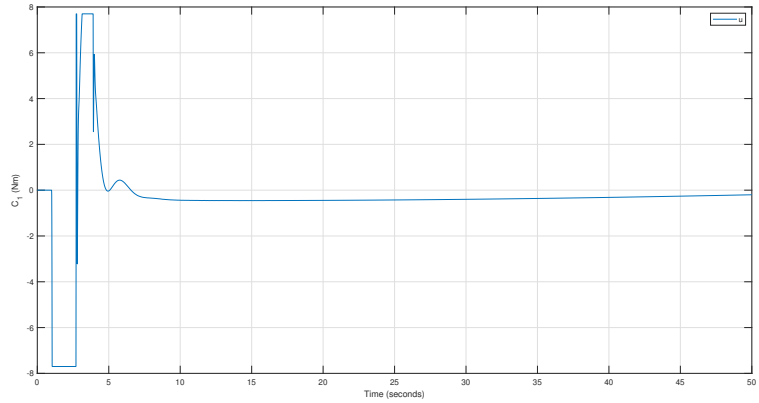


FIGURE 3.21: The control input to the system with a reference of 10m and no load with the anti-windup network

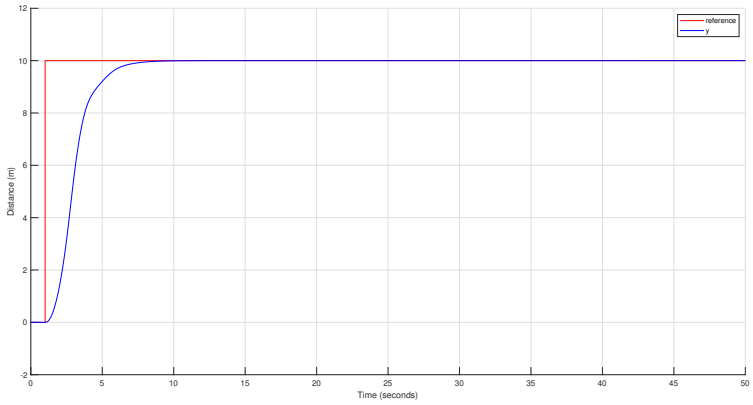


FIGURE 3.22: The step response of the system with a reference of 10m and no load with the anti-windup network

This final adjustment to the control scheme ensures a good step response in all case scenarios. Obviously, the higher the reference or the load, the worse will be the response, but all within a range of sufficient quality.

The final control scheme will be:

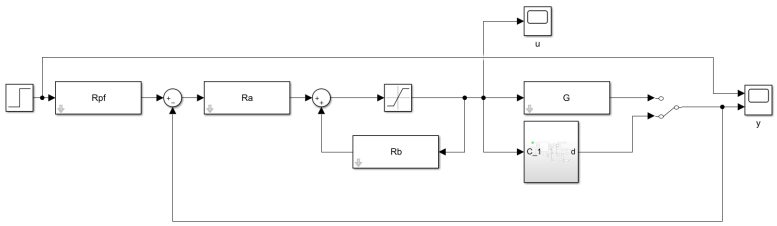


FIGURE 3.23: The Simulink configuration of the final control scheme for the fixed axes case

## 3.3 Control for the moving axes case

After designing the control system for the case where the relative position of the rotational axis of the two cylinders does not change in time, it is now necessary to consider the model closer to the reality, where the cylinder on top can actually fall down with respect to the lower body. Obviously this configuration presents several additional problems with respect to the previous one: the idea would be to keep the behaviour of the system as close as possible to the one before and to do so it is necessary to keep angle $\alpha$ as small as possible, ideally zero.

### 3.3.1 State space representation of the moving axes case

The first operation is as usual the creation of the state space representation of the system. Once again, to do so it is necessary to take into consideration the relations expressed in Equation (2.37), once again assuming only a pure rolling condition.

**Rearrangement of the dynamics equations with state variables**

The dynamics equations are:

$$\begin{cases} \ddot{\theta}_1 = \dfrac{C_1 - F_t r_1 + C_{rf_1} - W_{1tc} r_1}{J_1} \\ \ddot{\theta}_2 = \dfrac{-F_t r_2 + C_{rf_2} - W_{1tc} r_2}{J_2} \dfrac{W_{1n} r_2 \sin(\alpha)}{J_2 + m_2 {r_2}^2} \end{cases} \tag{3.53}$$

With:

$$F_t^\star = \frac{(C_1 + C_{rf_1} - W_{1tc} r_1) J_2 r_1 + (C_{rf_2} - W_{1tc} r_2) J_1 r_2 - W_{1n} \sin(\alpha) \dfrac{J_1 J_2 {r_2}^2}{J_2 + m_2 {r_2}^2}}{J_2 {r_1}^2 + J_1 {r_2}^2} \tag{3.54}$$

$$W_{1tc} = m_1 g \sin(\alpha) \tag{3.55}$$

$$W_{1n} = m_1 g \cos(\alpha) \tag{3.56}$$

Remember also that:

$$\alpha = \theta_1 \frac{r_1}{r_2} + \theta_2 - \frac{d_r}{r_2} + \arcsin\left( -\theta_2 \frac{r_2}{r_1 + r_2} + \sin(\alpha_0) \right) \tag{3.57}$$

and that:

$$d_r = \theta_1 r_1 + \theta_2 r_2 \tag{3.58}$$

The equations can be rewritten as:

$$\begin{cases} \ddot{\theta}_1 = & -m_1 g r_1 \left( \dfrac{1}{J_1} - \dfrac{J_2 {r_1}^2}{J_1 J_2 {r_1}^2 + {J_1}^2 {r_2}^2} - \dfrac{{r_2}^2}{J_2 {r_1}^2 + J_1 {r_2}^2} \right) \sin(\alpha) + \\ & + \dfrac{m_1 g J_1 J_2 r_1 {r_2}^2}{J_1 (J_2 {r_1}^2 + J_1 {r_2}^2)(J_2 + m_2 {r_2}^2)} \cos(\alpha) \sin(\alpha) + \\ & + \left( \dfrac{1}{J_1} - \dfrac{J_2 {r_1}^2}{J_1 J_2 {r_1}^2 + {J_1}^2 {r_2}^2} \right) C_{rf_1} - \dfrac{r_1 r_2}{J_2 {r_1}^2 + J_1 {r_2}^2} C_{rf_2} + \\ & + \left( \dfrac{1}{J_1} - \dfrac{J_2 {r_1}^2}{J_1 J_2 {r_1}^2 + {J_1}^2 {r_2}^2} \right) C_1 \\ \ddot{\theta}_2 = & -m_1 g r_2 \left( \dfrac{1}{J_2} - \dfrac{{r_1}^2}{J_2 {r_1}^2 + J_1 {r_2}^2} - \dfrac{J_1 {r_2}^2}{{J_2}^2 {r_1}^2 + J_1 J_2 {r_2}^2} \right) \sin(\alpha) - \\ & - m_1 g r_2 \left( \dfrac{1}{J_2 + m_2 {r_2}^2} - \dfrac{J_1 J_2 {r_2}^2}{J_2 (J_2 {r_1}^2 + J_1 {r_2}^2)(J_2 + m_2 {r_2}^2)} \right) \cos(\alpha) \sin(\alpha) - \\ & - \dfrac{r_1 r_2}{J_2 {r_1}^2 + J_1 {r_2}^2} C_{rf_1} + \left( \dfrac{1}{J_2} - \dfrac{J_1 {r_2}^2}{{J_2}^2 {r_1}^2 + J_1 J_2 {r_2}^2} \right) C_{rf_2} - \\ & - \dfrac{r_1 r_2}{J_2 {r_1}^2 + J_1 {r_2}^2} C_1 \end{cases} \tag{3.59}$$

Once again, for control model purposes, it is possible to treat the two rolling friction forces as standard dissipative forces in the form $\beta\dot{\theta}$:

$$C_{rf_1} = -\beta \dot{\theta}_1 \tag{3.60}$$

$$C_{rf_2} = -\beta \dot{\theta}_2 \tag{3.61}$$

This time, together with the output representing the horizontal position of the center of mass of the second cylinder $d = r_2 \theta_2$, we consider also a second output to

ensure the equilibrium of the first cylinder on top of the second one. This condition is represented by the angle $\alpha$ and therefore the second output will be:

$$\alpha = \theta_1 \frac{r_1}{r_2} + \theta_2 - \frac{d_r}{r_2} + \arcsin\left(-\theta_2 \frac{r_2}{r_1 + r_2} + \sin(\alpha_0)\right) \tag{3.62}$$

Now, the states and input to the system are once again defined as:

$$x_1 = \theta_1 \qquad x_2 = \dot{\theta}_1 \qquad x_3 = \theta_2 \qquad x_4 = \dot{\theta}_2 \qquad u = C_1 \tag{3.63}$$

Therefore, the state space representation of the system will be:

$$\begin{cases}
\dot{x}_1 = & x_2 \\
\dot{x}_2 = & -m_1 g r_1 \left(\frac{1}{J_1} - \frac{J_2 {r_1}^2}{J_1 J_2 {r_1}^2 + {J_1}^2 {r_2}^2} - \frac{{r_2}^2}{J_2 {r_1}^2 + J_1 {r_2}^2}\right) \\
& \sin\left(x_1 \frac{r_1}{r_2} + x_3 - \frac{x_1 r_1 + x_3 r_2}{r_2} + \arcsin\left(-x_3 \frac{r_2}{r_1 + r_2} + \sin(\alpha_0)\right)\right) + \\
& + \frac{m_1 g J_1 J_2 r_1 {r_2}^2}{J_1 (J_2 {r_1}^2 + J_1 {r_2}^2)(J_2 + m_2 {r_2}^2)} \\
& \cos\left(x_1 \frac{r_1}{r_2} + x_3 - \frac{x_1 r_1 + x_3 r_2}{r_2} + \arcsin\left(-x_3 \frac{r_2}{r_1 + r_2} + \sin(\alpha_0)\right)\right) \\
& \sin\left(x_1 \frac{r_1}{r_2} + x_3 - \frac{x_1 r_1 + x_3 r_2}{r_2} + \arcsin\left(-x_3 \frac{r_2}{r_1 + r_2} + \sin(\alpha_0)\right)\right) - \\
& - \beta \left(\frac{1}{J_1} - \frac{J_2 {r_1}^2}{J_1 J_2 {r_1}^2 + {J_1}^2 {r_2}^2}\right) x_2 + \frac{\beta r_1 r_2}{J_2 {r_1}^2 + J_1 {r_2}^2} x_4 + \\
& + \left(\frac{1}{J_1} - \frac{J_2 {r_1}^2}{J_1 J_2 {r_1}^2 + {J_1}^2 {r_2}^2}\right) u \\
\dot{x}_3 = & x_4 \\
\dot{x}_4 = & -m_1 g r_2 \left(\frac{1}{J_2} - \frac{{r_1}^2}{J_2 {r_1}^2 + J_1 {r_2}^2} - \frac{J_1 {r_2}^2}{{J_2}^2 {r_1}^2 + J_1 J_2 {r_2}^2}\right) \\
& \sin\left(x_1 \frac{r_1}{r_2} + x_3 - \frac{x_1 r_1 + x_3 r_2}{r_2} + \arcsin\left(-x_3 \frac{r_2}{r_1 + r_2} + \sin(\alpha_0)\right)\right) - \\
& - m_1 g r_2 \left(\frac{1}{J_2 + m_2 {r_2}^2} - \frac{J_1 J_2 {r_2}^2}{J_2 (J_2 {r_1}^2 + J_1 {r_2}^2)(J_2 + m_2 {r_2}^2)}\right) \\
& \cos\left(x_1 \frac{r_1}{r_2} + x_3 - \frac{x_1 r_1 + x_3 r_2}{r_2} + \arcsin\left(-x_3 \frac{r_2}{r_1 + r_2} + \sin(\alpha_0)\right)\right) \\
& \sin\left(x_1 \frac{r_1}{r_2} + x_3 - \frac{x_1 r_1 + x_3 r_2}{r_2} + \arcsin\left(-x_3 \frac{r_2}{r_1 + r_2} + \sin(\alpha_0)\right)\right) + \\
& + \frac{\beta r_1 r_2}{J_2 {r_1}^2 + J_1 {r_2}^2} x_2 - \beta \left(\frac{1}{J_2} - \frac{J_1 {r_2}^2}{{J_2}^2 {r_1}^2 + J_1 J_2 {r_2}^2}\right) x_4 - \\
& - \frac{r_1 r_2}{J_2 {r_1}^2 + J_1 {r_2}^2} u \\
y_1 = & r_2 x_3 \\
y_2 = & x_1 \frac{r_1}{r_2} + x_3 - \frac{x_1 r_1 + x_3 r_2}{r_2} + \arcsin\left(-x_3 \frac{r_2}{r_1 + r_2} + \sin(\alpha_0)\right)
\end{cases} \tag{3.64}$$

**Linearization of the system**

It is easy to see the system is highly non-linear, therefore a linearization [2] is in order. Intuitively, there is an unstable point of equilibrium for the system when both $\theta_1$ and $\theta_2$ are at zero degrees, the system is at rest and the input $C_1$ is null. Therefore it is possible to linearize the system for the equilibrium configuration $\bar{x} = [0\ 0\ 0\ 0]$

and $\bar{u} = [0]$. Notice that in this case $\alpha_0 = 0$ and, since pure rolling is assumed, $d_r = \theta_1 r_1 + \theta_2 r_2 = 0$.

Therefore, by calculating the partial derivative matrix for $\bar{x}$ and $\bar{u}$, the following $A$ matrix is obtained:

$$A = \begin{bmatrix} 0 & 1 & 0 & 0 \\ \left.\frac{\partial f_2}{\partial x_1}\right|_{\bar{x},\bar{u}} & \left.\frac{\partial f_2}{\partial x_2}\right|_{\bar{x},\bar{u}} & \left.\frac{\partial f_2}{\partial x_3}\right|_{\bar{x},\bar{u}} & \left.\frac{\partial f_2}{\partial x_4}\right|_{\bar{x},\bar{u}} \\ 0 & 0 & 0 & 1 \\ \left.\frac{\partial f_4}{\partial x_1}\right|_{\bar{x},\bar{u}} & \left.\frac{\partial f_4}{\partial x_2}\right|_{\bar{x},\bar{u}} & \left.\frac{\partial f_4}{\partial x_3}\right|_{\bar{x},\bar{u}} & \left.\frac{\partial f_4}{\partial x_4}\right|_{\bar{x},\bar{u}} \end{bmatrix} \tag{3.65}$$

with:

$$\begin{aligned}
\left.\frac{\partial f_2}{\partial x_1}\right|_{\bar{x},\bar{u}} =& g m_1 {r_1}^2 \left( -\frac{1}{J_1 r_2} + \frac{r_2}{J_2 {r_1}^2 + J_1 {r_2}^2} + \frac{J_2 {r_1}^2}{J_1 J_2 {r_1}^2 r_2 + {J_1}^2 {r_2}^3} + \right. \\
& \left. + \frac{J_2 r_2}{(J_2 {r_1}^2 + J_1 {r_2}^2)(J_2 + m_2 {r_2}^2)} \right) \\
\left.\frac{\partial f_2}{\partial x_2}\right|_{\bar{x},\bar{u}} =& -\beta \left( \frac{1}{J_1} - \frac{J_2 {r_1}^2}{J_1 J_2 {r_1}^2 + {J_1}^2 {r_2}^2} \right) \\
\left.\frac{\partial f_2}{\partial x_3}\right|_{\bar{x},\bar{u}} =& g m_1 r_1 \left( 1 - \frac{r_2}{r_1 + r_2} \right) \left( -\frac{1}{J_1} + \frac{{r_2}^2}{J_2 {r_1}^2 + J_1 {r_2}^2} + \frac{J_2 {r_1}^2}{J_1 J_2 {r_1}^2 + {J_1}^2 {r_2}^2} + \right. \\
& \left. + \frac{J_2 {r_2}^2}{(J_2 {r_1}^2 + J_1 {r_2}^2)(J_2 + m_2 {r_2}^2)} \right) \\
\left.\frac{\partial f_2}{\partial x_4}\right|_{\bar{x},\bar{u}} =& \frac{\beta r_1 r_2}{J_2 {r_1}^2 + J_1 {r_2}^2} \\
\left.\frac{\partial f_4}{\partial x_1}\right|_{\bar{x},\bar{u}} =& -g m_1 r_1 \left( \frac{1}{J_2} - \frac{{r_1}^2}{J_2 {r_1}^2 + J_1 {r_2}^2} - \frac{J_1 {r_2}^2}{{J_2}^2 {r_1}^2 + J_1 J_2 {r_2}^2} + \frac{1}{J_2 + m_2 {r_2}^2} - \right. \\
& \left. - \frac{J_1 {r_2}^2}{J_2 (J_2 {r_1}^2 + J_1 {r_2}^2)(J_2 + m_2 {r_2}^2)} \right) \\
\left.\frac{\partial f_4}{\partial x_2}\right|_{\bar{x},\bar{u}} =& \frac{\beta r_1 r_2}{J_2 {r_1}^2 + J_1 {r_2}^2} \\
\left.\frac{\partial f_4}{\partial x_3}\right|_{\bar{x},\bar{u}} =& -g m_1 r_2 \left( 1 - \frac{r_2}{r_1 + r_2} \right) \left( \frac{1}{J_2} - \frac{{r_1}^2}{J_2 {r_1}^2 + J_1 {r_2}^2} - \frac{J_1 {r_2}^2}{{J_2}^2 {r_1}^2 + J_1 J_2 {r_2}^2} + \right. \\
& \left. + \frac{1}{J_2 + m_2 {r_2}^2} - \frac{J_1 {r_2}^2}{J_2 (J_2 {r_1}^2 + J_1 {r_2}^2)(J_2 + m_2 {r_2}^2)} \right) \\
\left.\frac{\partial f_4}{\partial x_4}\right|_{\bar{x},\bar{u}} =& -\beta \left( \frac{1}{J_2} - \frac{J_1 {r_2}^2}{{J_2}^2 {r_1}^2 + J_1 J_2 {r_2}^2} \right)
\end{aligned} \tag{3.66}$$

The other matrices then are:

$$B = \begin{bmatrix} 0 \\ \dfrac{1}{J_1} - \dfrac{J_2 {r_1}^2}{J_1 J_2 {r_1}^2 + {J_1}^2 {r_2}^2} \\ 0 \\ -\dfrac{r_1 r_2}{J_2 {r_1}^2 + J_1 {r_2}^2} \end{bmatrix} \tag{3.67}$$

$$C = \begin{bmatrix} 0 & 0 & r_2 & 0 \\ \dfrac{r_1}{r_2} & 0 & 1 - \dfrac{r_2}{r_1 + r_2} & 0 \end{bmatrix} \tag{3.68}$$

$$D = \begin{bmatrix} 0 \\ 0 \end{bmatrix} \tag{3.69}$$

The previous arbitrary quantities are now assigned to find the numerical value for the matrices:

$$m_1 = 5\,kg \tag{3.70}$$
$$m_2 = 20\,kg \tag{3.71}$$
$$r_1 = 0.2\,m \tag{3.72}$$
$$r_2 = 0.5\,m \tag{3.73}$$
$$J_1 = \frac{1}{2} m_1 {r_1}^2 = 0.1\,kg \times m^2 \tag{3.74}$$
$$J_2 = \frac{1}{2} m_2 {r_2}^2 = 2.5\,kg \times m^2 \tag{3.75}$$
$$\beta = 0.0065 \tag{3.76}$$

Therefore:

$$A = \begin{bmatrix} 0 & 1 & 0 & 0 \\ 2.616 & -0.013 & 1.8686 & 0.0052 \\ 0 & 0 & 0 & 1 \\ -1.2034 & 0.0052 & -0.8595 & -0.0021 \end{bmatrix} \tag{3.77}$$

$$B = \begin{bmatrix} 0 \\ 2 \\ 0 \\ -0.8 \end{bmatrix} \tag{3.78}$$

$$C = \begin{bmatrix} 0 & 0 & 0.5 & 0 \\ 0.4 & 0 & 0.2857 & 0 \end{bmatrix} \tag{3.79}$$

$$D = \begin{bmatrix} 0 \\ 0 \end{bmatrix} \tag{3.80}$$

This time, however, it is easy to see that the system is not SISO. In fact, together with the output $d = r_2\theta_2$ indicating the horizontal position of the center of mass of the second cylinder, there is the second output $\alpha = \theta_1 \frac{r_1}{r_2} + \theta_2 + \arcsin\left(-\theta_2 \frac{r_2}{r_1 + r_2}\right)$ indicating the relative angular position of the two rotational axis.

For this reason, a single transfer function cannot be defined from the state matrices. Instead, a transfer matrix could be defined, meaning a matrix whose elements are transfer functions:

$$H(s) = \begin{bmatrix} -0.4 \dfrac{s^2 + 0.3925}{(s+1.333)(s-1.317)(s+0.0119)(s+0.0106)} \\ 0.5714 \dfrac{(s+0104)(s-0.0104)}{(s+1.333)(s-1.317)(s+0.0119)(s+0.0106)} \end{bmatrix} \tag{3.81}$$

However, this structure becomes complicated to handle in terms of control. For this reason, this control design will consider a different approach with respect to the previous one.

Since the position control of the system was thoroughly analysed in the previous section, the following analysis will be more dedicated to the stabilization of the system when it faces initial condition different from the vertical configuration. If, for example, the top cylinder starts from a position where it is already slightly falling, the system should be able to stabilize and go to the vertical configuration.

### 3.3.2 Controller design for the moving axes case

#### Stability analysis of the autonomous case

Remember that the system was linearized for a point of equilibrium with $\bar{x} = [0\,0\,0\,0]$ and $\bar{u} = [0]$. It is easy to imagine that this point of equilibrium is highly unstable, since a small variation on any state would cause the top cylinder to fall, influencing both outputs and increasing their value indefinitely (in reality $\alpha$ is bounded since after a certain value of alpha the two cylinders would detach).

To confirm this intuition, it is possible to analyze the response of the system when imposing an initial value of $\theta_{10} = \dfrac{\pi}{10} = 0.3142\,rad$

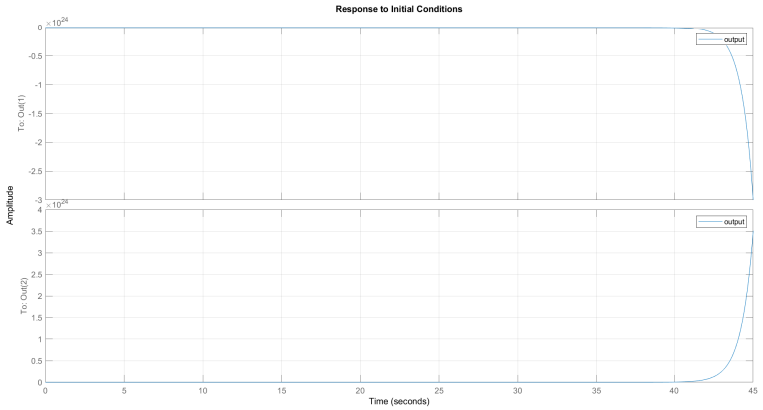


FIGURE 3.24: The value of $d$ and $\alpha$ for $\theta_{10} = \frac{\pi}{10}$

As can be seen the system is unstable for both $d$ (upper graph) and $\alpha$ (lower graph).

The reason for this can be found by analyzing the eigenvalues for the $A$ matrix:

$$\begin{aligned} \lambda_{A1} &= -1.3335 \\ \lambda_{A2} &= +1.3171 \\ \lambda_{A3} &= +0.0119 \\ \lambda_{A4} &= -0.0106 \end{aligned} \tag{3.82}$$

As expected, at least one of the eigenvalues, representing the position of the poles of the open loop system, has positive real part, making the system unstable. In order to stabilize the system, these poles must therefore be moved to the left half of the plane.

### Pole placement

A powerful technique to do this is called pole placement [6]. This procedure, differently from a standard controller in frequency domain, does not act on the output of the plant to generate a control input. Instead, it works directly on the states of the system, which is a perfect fit for this situation since the system is only defined in state space.

In particular, the idea is to multiply the state vector of the system by a matrix made up of a set of gain values, then subtract the result from the reference signal and feed the difference back in the plant. This gain matrix $K$ allows to move the poles of the closed loop system (indicated by the eigenvalues of matrix $A$) to a desired location that satisfies the requirements.

The desired position of the poles for the closed loop system can be chosen arbitrarily for the moment, depending on the wanted performances of the system.

For the moment, the first attempt will be made by moving the two positive poles to the negative plane by just inverting their sign.

Therefore, the final desired eigenvalues are:

$$\begin{aligned} \lambda_{A1} &= -1.3335 \\ \lambda_{A2} &= -1.3171 \\ \lambda_{A3} &= -0.0119 \\ \lambda_{A4} &= -0.0106 \end{aligned} \tag{3.83}$$

In order to move the poles to the required position, the Matlab instruction place$(A, B, P)$ (where $P$ is the vector of the desired eigenvalues) can be used as it directly calculates the required values for the $K$ matrix. In this case the matrix is:

$$K = \begin{bmatrix} 2.5000 & 1.7931 & 1.7844 & 1.1603 \end{bmatrix} \tag{3.84}$$

By implementing this regulator, the step response of the system becomes:

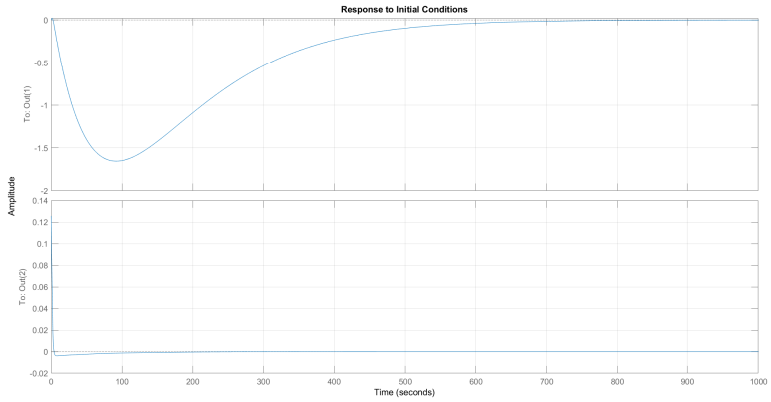


FIGURE 3.25: The response of the system for $\theta_{10} = \dfrac{\pi}{10}$ with the implementation of the first matrix $K$ by pole placement

Even if the overshoot is really small, it is easy to see the settling time is far too big.

In order to try and solve this problem, an idea could be moving the poles to a higher frequency in order to make the system faster. For this reason the previous operation is repeated with desired eigenvalues:

$$\begin{aligned} \lambda_{A1} &= -133.35 \\ \lambda_{A2} &= -131.71 \\ \lambda_{A3} &= -1.19 \\ \lambda_{A4} &= -1.06 \end{aligned} \tag{3.85}$$

Now the $K$ matrix becomes:

$$K = \begin{bmatrix} -26787 & -70868 & -89676 & -177500 \end{bmatrix} \tag{3.86}$$

And the response is:

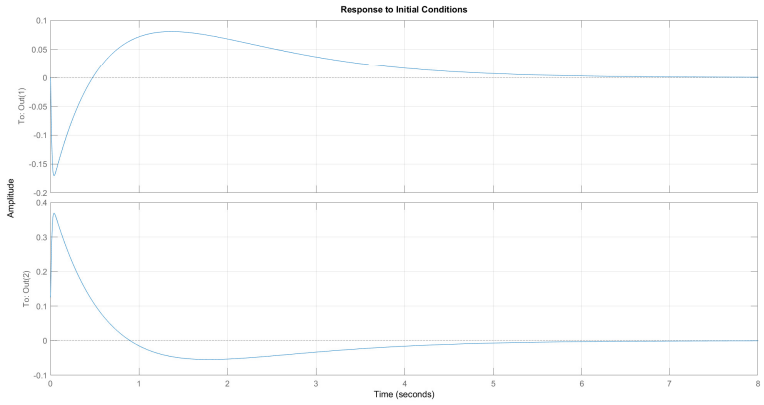


FIGURE 3.26: The response of the system for $\theta_{10} = \frac{\pi}{10}$ with the implementation of the second matrix $K$ by pole placement

Even though now the response is pretty good, with settling time below 10 seconds, this result requires an extremely high gain (order of $10^5$) and is therefore not ideal.

In order to try and find a compromise between a good response and a reduced effort, a more advanced technique should be implemented.

### LQR

The previous control technique is potentially really powerful, since it makes it very easy to stabilize a system by simply placing its closed-loop poles. The problem, however, comes with the quality of the response. If a specific characteristic of the response (limitation on the input, reduced overshoot on the output,...) has particular importance, it is extremely difficult to control it by simply deducing the ideal position of the poles. In order not to need a long process of trial and error, a more evolved technique has been introduced.

The LQR (Linear Quadratic Regulator) [7] [8] is a form of optimal control used to have a more intuitive way to manipulate the characteristics of the desired response of the system.

Very briefly, the algorithm uses a "cost function" in order to determine the best values of $K$ based on the requirements of the project. The cost function is:

$$J = \int_0^\infty (x^T Q x + u^T R u)\, dt \tag{3.87}$$

where the term $x^T Q x$ can be seen as the "performance factor" and the term $u^T R u$ represents the "effort factor". By solving the LQR problem, the relation:

$$u = -Kx \tag{3.88}$$

is obtained. From this relation the optimal gain matrix $K$ can be found.

Since the main object of this part is the control of the outputs, rather than the states, a small variation to the formula will be made by substituting the performance matrix $Q$ with the matrix $C^T Q C$. Thanks to this choice, it is possible to weigh the output of the system by confronting them with the control signal.

In order to find a starting point for this method, a possibility is to first initialize both matrices $Q$ and $R$ to the identity value.

Since it is weighed on the outputs, the performance matrix $Q$ will be a 2x2:

$$Q = \begin{bmatrix} 1 & 0 \\ 0 & 1 \end{bmatrix} \tag{3.89}$$

The effort matrix $R$, instead, will be a 1x1 since the system is single-input:

$$R = \begin{bmatrix} 1 \end{bmatrix} \tag{3.90}$$

By now solving the LQR problem with these two matrices, the value for $K$ becomes:

$$K = \begin{bmatrix} 3.0222 & 0.5434 & 1.6578 & -2.4624 \end{bmatrix} \tag{3.91}$$

By implementing this new gain matrix in the state feedback loop as was done for the pole placement technique, the following results are obtained:

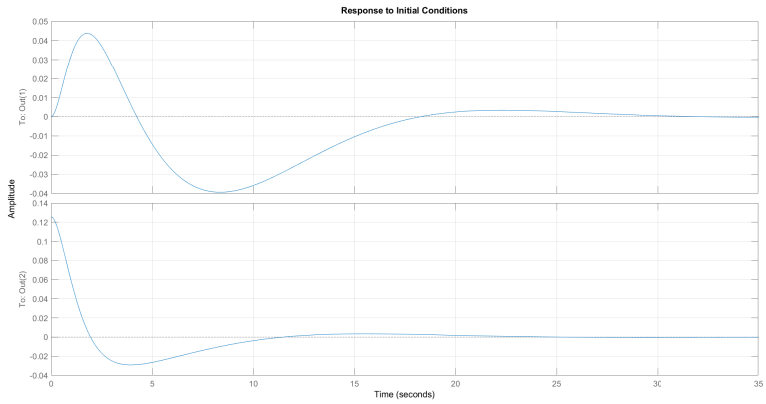


FIGURE 3.27: The response of the system for $\theta_{10} = \frac{\pi}{10}$ with the implementation of matrix $K$ for $Q = 1$

By chance, with the first arbitrary attempt made of two identity matrices $Q$ and $R$, the response looks valid. In fact, the overshoot is very low, the settling time is not excessive and, moreover, the gain is much lower than the previous case of pole placement.

Concerning the linearized system, it can be said that this regulator works fine for this project requirements.

### 3.3.3 Implementation on real system for the moving axes case

#### LQR implementation

As was said, as long as a linearized system is considered, the previous regulator works fine, since it is able to stabilize the system after an initial offset.

Now it is time to apply the regulator to the real system, obtaining the following response (only $\alpha$ will be considered for now):

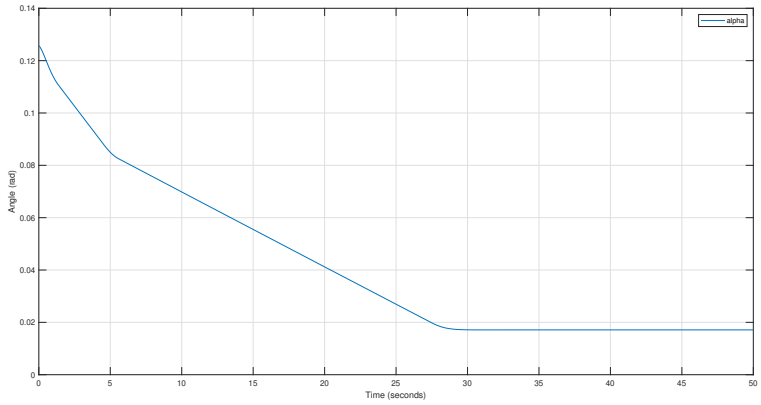


FIGURE 3.28: The response of the real system for $\theta_{10} = \frac{\pi}{10}$ with the implementation of matrix $K$ for $Q = 1$

There are two main problems in this response.

The first is that the value of $\alpha$ does not go to zero at steady state, but instead stabilizes on a slightly higher value. This problem will be dealt with later.

The second problem is that the setting time is visibly worse than the linearized case, with the response that settles after about 30 seconds. For this second issue, a controller modification can be implemented through LQR.

In fact, if before the identity matrix $Q$ and $R$ fit perfectly, this time a faster response is desired. for this reason the value of matrix $Q$ is increased to:

$$Q = \begin{bmatrix} 10^3 & 0 \\ 0 & 10^3 \end{bmatrix} \tag{3.92}$$

And the response thus becomes:

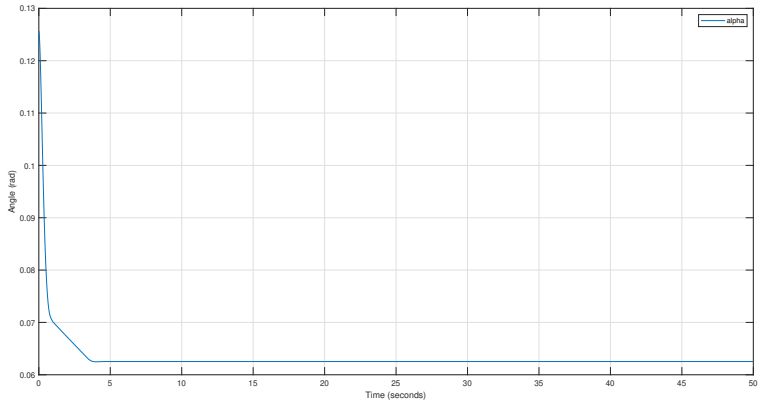


FIGURE 3.29: The response of the real system for $\theta_{10} = \frac{\pi}{10}$ with the implementation of matrix $K$ for $Q = 10^3$

Which is much faster than before.

Notice also that the matrix $K$ for this case is:

$$K = \begin{bmatrix} 10.1604 & -14.9231 & -8.5586 & -46.5030 \end{bmatrix} \tag{3.93}$$

that is not too big even though the response is quite fast.

### Input variable considerations

An important point to be careful with when dealing with the real system is the control input $u$ to the system. As for the fixed axes case, this input corresponds to the driving torque $C_1$ and must, therefore, generated a transmission force that must be lower than the value of the static friction force.

In the case that was just analysed, the value of $u$ was:

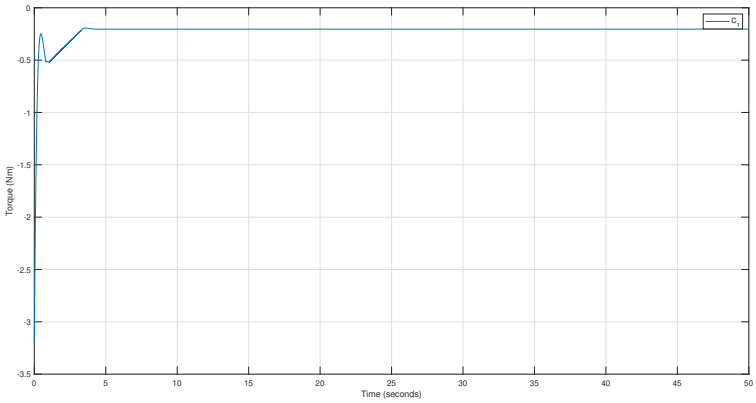


FIGURE 3.30: The value of $u$ for the real system for $\theta_{10} = \dfrac{\pi}{10}$ with the implementation of matrix $K$ for $Q = 10^3$

It reaches a minimum value of around $-3.2\,N$ that keeps the system in pure rolling.

If, however, the initial offset is increased at, for instance, $\theta_{10} = \dfrac{\pi}{3}$, the following situation occurs:

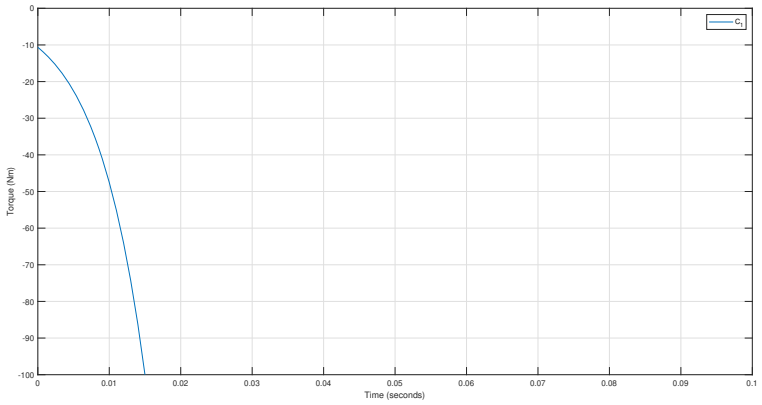


FIGURE 3.31: The value of $u$ for the real system for $\theta_{10} = \frac{\pi}{3}$ with the implementation of matrix $K$ for $Q = 10^3$

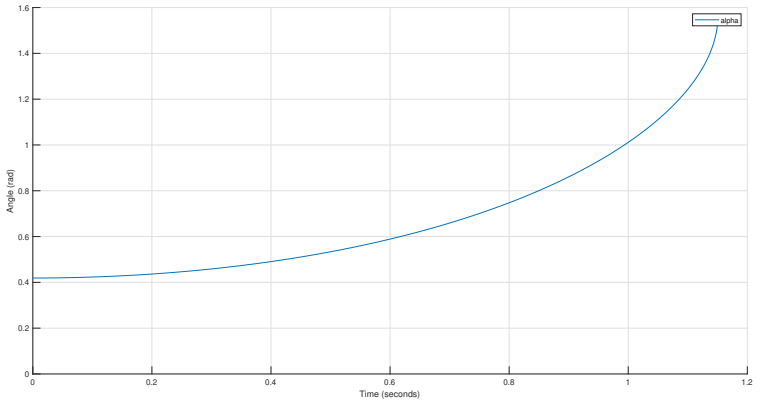


FIGURE 3.32: The response of the real system for $\theta_{10} = \frac{\pi}{3}$ with the implementation of matrix $K$ for $Q = 10^3$

In this case, the initial torque the system provides to cope with the offset is too great and brings the dynamics to rolling with sliding. From this moment on, the input signal does not have a direct effect on the system and the top cylinder keeps sliding down the bottom one. Moreover, since the regulator understands that the system is moving away from the point of equilibrium, it keeps increasing the input torque in the attempt to solve the situation. This action, however, only worsens the scenario since it will be farther from going back to a pure rolling situation.

In order to prevent this kind of situation from happening, a limitation to the input torque must be introduced.

### 3.3.4 Implementation of saturation

If in the fixed axis case a prefilter was used in order to limit the control input, that time the system was responding to a step reference. In this case, instead, there is no reference and the system must only be able to return to its equilibrium configuration. For this reason a prefilter, that filters out the higher frequencies of a step reference, is completely useless.

On the other hand, another tool of which great use was made in the previous design was the saturation. The problem with saturation was that it tended to slow down the system a lot due to the windup phenomenon and therefore an anti-windup network was necessary. In this case, though, since the movements to be performed are conceptually very small, even if the system is a bit slower, but eventually reaches the steady state without applying too much torque, the solution is undoubtedly preferable. For this reason, a saturation is introduced in the system to limit the control input.

As for the previous case, the saturation value should be chosen based on the system parameters so as not to allow an input to the system that would bring it to a sliding dynamics. This time, however, having a variable normal force $W_1 \cos(\alpha)$ it is not possible to cover all system configurations: for example, for $\alpha = \frac{\pi}{2}$ the static friction force is null and therefore no coupling is possible at all. For this reason it is necessary to define a limited range for $\alpha$ that will be considered for the analysis.

A suitable value would be the range that spans from $\alpha = -\frac{\pi}{4}$ and $\alpha = \frac{\pi}{4}$.

Once again the fundamental relation is the one written in Equation (2.38):

$$|F_t + W_{1t}| < \mu_s W_1 \cos(\alpha) \tag{3.94}$$

that must be calculated for $\alpha \pm \frac{\pi}{4}$ in order to find the worst case scenarios. By following the procedure that was illustrated in the previous case (Equation (3.47)) and considering both the cases with $\alpha \pm \frac{\pi}{4}$ and taking the most strict conditions, the following upper and lower bounds are found:

$$\begin{cases} C_1 > -6.08475 \\ C_1 < 6.08475 \end{cases} \tag{3.95}$$

Therefore for this case the two values for the saturation will be:

$$C_{1max} = 6.0\ Nm \tag{3.96}$$

$$C_{1min} = -6.0\ Nm \tag{3.97}$$

Notice that these two values are lower than those for the horizontal case since here it is easier to overcome the static friction value due to the normal force decreasing with the rotational axis movement.

By implementing the saturation on the real system, it is possible to see how the previous case with $\theta_{10} = \frac{\pi}{3}$ that would bring the system to instability is now managed by the controller.

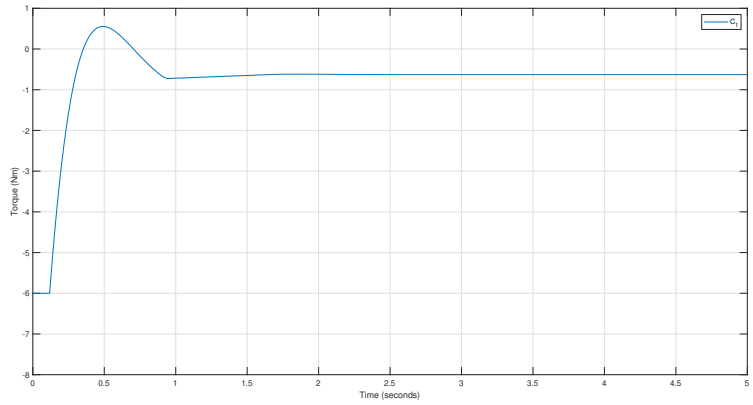


FIGURE 3.33: The value of $u$ for the real system for $\theta_{10} = \frac{\pi}{3}$ with the implementation of matrix $K$ for $Q = 10^3$ and saturation

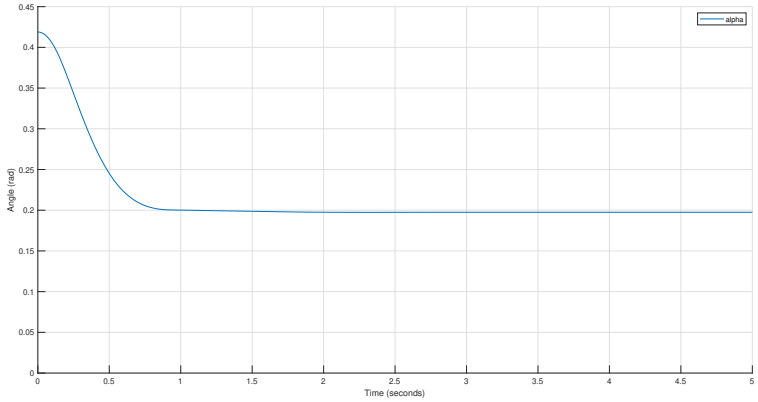


FIGURE 3.34: The response of the real system for $\theta_{10} = \frac{\pi}{3}$ with the implementation of matrix $K$ for $Q = 10^3$ and saturation

Thanks to saturation now the system is able to cope with bigger initial offsets. Obviously if the initial offset is too big, for example so that $\alpha = \frac{\pi}{2}$, there is nothing the system can do.

Now the only problem left to solve is the steady state error on the value of $\alpha$.

### 3.3.5 Integration of the steady state error

Since the controller was initially designed referring to the linearized system, it could not take into account some parameters that were derived during linearization. For this reason, although a stability is reached thanks to the controller, there is a constant steady state error.

In order to solve this problem, the first solution that comes to mind is using an integrator that brings the steady state error to zero.

Therefore, the system with the LQR controller can be seen as a sort of stabilized inner loop, to which an outer loop is applied. This time, since it is a frequency domain standard control, the information fed back into the system is the output angle $\alpha$ rather than the states of the system.

By adding a simple integrator in the outer loop, the response of the system is:

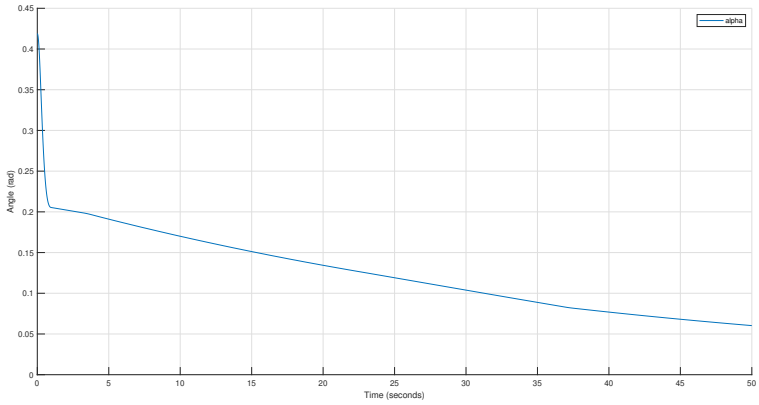


FIGURE 3.35: The response of the real system for $\theta_{10} = \frac{\pi}{3}$ with the previous control system and an integrator (gain 1)

It is possible to see that the value of $\alpha$ is indeed falling towards zero, but it is doing so at an extremely low pace since the system is very slow.

In order to speed up the response, a simple arbitrary gain is added so that the final regulator is:

$$R(s) = \frac{30}{s} \tag{3.98}$$

By implementing this new regulator in the outer loop of the system, the response becomes:

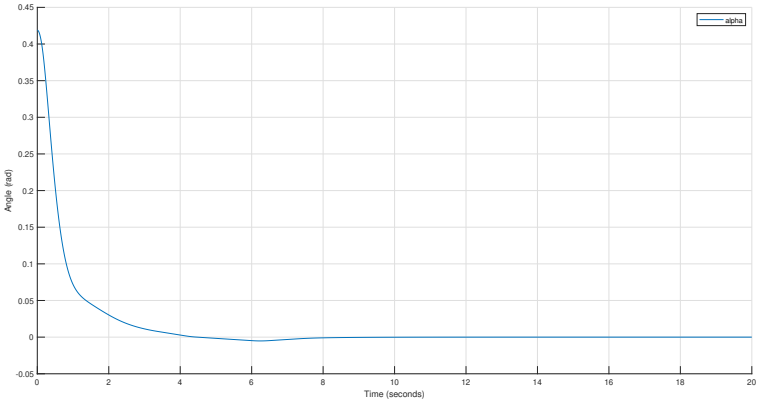


FIGURE 3.36: The response of the real system for $\theta_{10} = \frac{\pi}{3}$ with the previous control system and an integrator (gain 30)

The response now has zero steady state error, minimum overshoot and a settling time below 10 seconds.

The final control scheme will be:

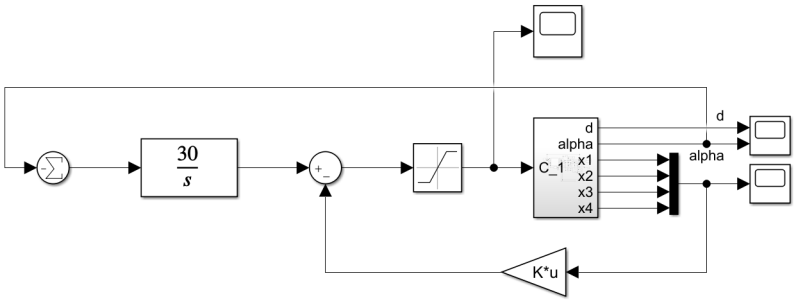


FIGURE 3.37: The Simulink configuration of the final control scheme for the moving axes case

# Chapter 4

# Future Developments

## 4.1 Introduction

This brief chapter is introduced in order to suggest possible future developments based on this work. In particular, the two main topics will be an optimization of the work, in terms of model and control, and an expansion of the work, adding more parts and functionalities.

The goal would be, ideally, to arrive at the final result of a well modelled and fully functioning Ball-Balancing Robot.

## 4.2 Optimization

### 4.2.1 Carter's analysis on micro slip

This part of the optimization is strictly related to the modelling of the system. In particular it refers to a better and more precise way to describe the passage from a pure rolling condition to a rolling with sliding one.

In this work, the transition from pure rolling to rolling with sliding has been described as an abrupt passage. As with all real phenomena this is actually a simplification.

A better description of the behaviour was made in 1926 by F. W. Carter in his treaty *Action of a Locomotive Driving Wheel* [3] where the author analyses the behaviour of a wheel on a rail along the longitudinal direction. Later studies then amplified the matter by analysing also the transverse direction thus concerning the 3-D space. To carry out this study it has been assumed to treat the wheels of the train and the rails (that have a slight curvature) as a couple of cylinders in contact, therefore making the study applicable to our case.

Carter explains that bodies in contact have a peculiar interaction, called micro slip, as their area of contact (in an ideal case it would be a single point, but due to deformation it becomes more extended in a real environment) is divided in two smaller regions: the stick region and the slip region. The sliding occurs only in the slip region, while in the stick region corresponding material points remain in contact. It is suggested that in the ideal case of pure rolling, the stick region covers the whole area, the contrary occurs in the event of sliding. As a consequence, the total tangential traction force over the contact area strongly depends on the proportion between the stick and the slip region.

This model allows to obtain a smoother transition from pure rolling to rolling with sliding thanks to the analysis of the stick and the slip region.

### 4.2.2 Rolling with sliding with the ground

In this work, when dealing with the moving axes case, a pure rolling with the ground has been assumed for simplicity. However, depending mostly on the friction coefficient between the bottom cylinder and the plane, a sliding condition may occur.

In that case, a further limitation on the control input should be considered so that the force transmitted from the bottom cylinder to the ground does not overcome the static friction one.

### 4.2.3 Other modelling optimizations

Other little elements can be introduced in the model in order to make it as realistic as possible. Some may be:

- rolling friction between the bottom cylinder and the ground
- friction in the top cylinder's rotation axis
- air resistance

All these elements, although acknowledged, have been neglected in order to simplify the model.

### 4.2.4 Optimization of the controllers

In this work the controllers' parameters have been chosen more or less arbitrarily mostly without real specifics in mind.

In general, when the control should be applied to a real case much more information come into play, both in terms of required performance and controller system limitations (actuators, sensors,...).

For these reasons, a more optimized design of the controllers should be carried out in order to meet the required performances while minimizing the control system efforts.

## 4.3 Expansion

### 4.3.1 Addition of an inverted pendulum

This work was mainly focused on the model and control of the rolling dynamics between a wheel and a lower cylinder. In particular, the wheel has been assumed as the whole body of the robot, with its mass depending only on the mass of the wheel. Obviously, the real case is quite far from this, since the body of the robot must include all the actuators, sensors, cabling,... and is therefore a complex structure.

The best way to model this body, as for the Self-Balancing Robot case, is by means of an inverted pendulum. This model should be added to the previous model in order to obtain, in other words, a sort of Self-Balancing Robot balancing on a cylinder.

Regarding the modelling of the pendulum, a possible state space model was done during the creation of this thesis. It will be now briefly showed.

The dynamics equations are:

$$(M+m)\ddot{s} + m\frac{l}{2}\ddot{\theta}\cos\theta = m\frac{l}{2}\dot{\theta}^2\sin\theta - ks - \beta_1\dot{s} + F - F_d \tag{4.1}$$

$$m\frac{l}{2}\cos\theta\ddot{s} + (J_P + m\frac{l^2}{4})\ddot{\theta} = mg\frac{l}{2}\sin\theta - F_d\frac{l}{2}\cos\theta - \beta_2\dot{\theta} \tag{4.2}$$

with:

$$\begin{aligned}
s &\rightarrow \text{linear position of the kart} \\
\theta &\rightarrow \text{angular position of the pendulum} \\
M &\rightarrow \text{mass of the kart} \\
m &\rightarrow \text{mass of the pendulum} \\
l &\rightarrow \text{length of the pendulum} \\
J_P &\rightarrow \text{moment of inertia of the pendulum} \\
k &\rightarrow \text{elastic force coefficient on the kart} \\
\beta_1 &\rightarrow \text{kart viscous friction coefficient} \\
\beta_2 &\rightarrow \text{pendulum viscous friction coefficient} \\
F &\rightarrow \text{input force applied on the kart} \\
F_d &\rightarrow \text{disturbance force applied on the pendulum}
\end{aligned} \tag{4.3}$$

Now, the system can be written in state space representation with:

$$x_1 = s \qquad x_2 = \dot{s} \qquad x_3 = \theta \qquad x_4 = \dot{\theta} \qquad u_1 = F \qquad u_2 = F_d \tag{4.4}$$

To simplify the writing, some new parameters are introduced. For what concerns the first equation:

$$a_1 = M + m \qquad b_1 = m\frac{l}{2} \qquad c_1 = k \qquad d_1 = \beta_1 \tag{4.5}$$

While for the second equation:

$$a_2 = b_1 = m\frac{l}{2} \qquad b_2 = J_G + m\frac{l^2}{4} \qquad c_2 = mg\frac{l}{2} \qquad d_2 = \frac{l}{2} \qquad e_2 = \beta_2 \tag{4.6}$$

The state space model thus becomes:

$$\begin{cases}
\dot{x}_1 = x_2 \\
\dot{x}_2 = -\dfrac{b_2 c_1}{a_1 b_2 - b_1^2 \cos^2 x_3} x_1 - \dfrac{b_2 d_1}{a_1 b_2 - b_1^2 \cos^2 x_3} x_2 + \dfrac{b_1 e_2 \cos x_3}{a_1 b_2 - b_1^2 \cos^2 x_3} x_4 + \\
\quad + \dfrac{b_1 b_2 \sin x_3}{a_1 b_2 - b_1^2 \cos^2 x_3} x_4^2 + \dfrac{b_2}{a_1 b_2 - b_1^2 \cos^2 x_3} u_1 - \dfrac{b_2 - b_1 d_2 \cos^2 x_3}{a_1 b_2 - b_1^2 \cos^2 x_3} u_2 - \\
\quad - \dfrac{b_1 c_2 \cos x_3 \sin x_3}{a_1 b_2 - b_1^2 \cos^2 x_3} \\
\dot{x}_3 = x_4 \\
\dot{x}_4 = \dfrac{b_1 c_1 \cos x_3}{a_1 b_2 - b_1^2 \cos^2 x_3} x_1 + \dfrac{b_1 d_1 \cos x_3}{a_1 b_2 - b_1^2 \cos^2 x_3} x_2 - \dfrac{a_1 e_2}{a_1 b_2 - b_1^2 \cos^2 x_3} x_4 - \\
\quad - \dfrac{b_1^2 \cos x_3 \sin x_3}{a_1 b_2 - b_1^2 \cos^2 x_3} x_4^2 - \dfrac{b_1 \cos x_3}{a_1 b_2 - b_1^2 \cos^2 x_3} u_1 + \\
\quad + \dfrac{b_1 \cos x_3 - a_1 d_2 \cos x_3}{a_1 b_2 - b_1^2 \cos^2 x_3} u_2 + \dfrac{a_1 c_2 \sin x_3}{a_1 b_2 - b_1^2 \cos^2 x_3}
\end{cases} \tag{4.7}$$

By linearizing the system around the point of equilibrium $\bar{x} = [0\ 0\ 0\ 0]$ and $\bar{u} = [0\ 0]$ the following $A$ matrix is obtained:

$$A = \begin{bmatrix} 0 & 1 & 0 & 0 \\ -\frac{b_2 c_1}{a_1 b_2 - b_1^2} & -\frac{b_2 d_1}{a_1 b_2 - b_1^2} & -\frac{b_1 c_2}{a_1 b_2 - b_1^2} & \frac{b_1 e_2}{a_1 b_2 - b_1^2} \\ 0 & 0 & 0 & 1 \\ \frac{b_1 c_1}{a_1 b_2 - b_1^2} & \frac{b_1 d_1}{a_1 b_2 - b_1^2} & \frac{a_1 c_2}{a_1 b_2 - b_1^2} & -\frac{a_1 e_2}{a_1 b_2 - b_1^2} \end{bmatrix} \tag{4.8}$$

By assigning the following arbitrary values to the system: Now we assign some symbolic values to the pendulum:

$$\begin{aligned} M &= 1\,Kg \\ m &= 0.5\,Kg \\ l &= 0.3\,m \\ J_G &= 3.75 \times 10^{-3}\,Kg \times m^2 \\ K &= 10\,N/m \\ \beta_1 &= 5.0 \times 10^{-3}\,Pa \times s \\ \beta_2 &= 5.0 \times 10^{-3}\,Pa \times s \\ g &= 9.81\,m/s^2 \end{aligned} \tag{4.9}$$

the $A$ matrix becomes:

$$A_0 = \begin{bmatrix} 0 & 1.0000 & 0 & 0 \\ -7.7778 & -0.0039 & -1.6350 & 0.0111 \\ 0 & 0 & 0 & 1.0000 \\ 22.2222 & 0.0111 & 32.7000 & -0.2222 \end{bmatrix} \tag{4.10}$$

and its eigenvalues are:

$$\begin{aligned} \lambda_{A1} &= -5.7494 + 0.0000i \\ \lambda_{A2} &= +5.5279 + 0.0000i \\ \lambda_{A3} &= -0.0023 + 2.6190i \\ \lambda_{A4} &= -0.0023 - 2.6190i \end{aligned} \tag{4.11}$$

that show an expected instability of the point of equilibrium due to the second eigenvalue having positive real part.

### 4.3.2 Modelling of the motor

Together with the mechanical modelling of the system, for the final realization of a functioning robot, also a model of the used motor is required.

In particular this model should show the correlation between the main electrical quantities (voltage and current) and the torque actually applied by the motor. This relation mostly depends on the type of motor used (most probably electrical) the inverter and the reduction gear.

### 4.3.3 Combination of the two controls

The control part was split into two analyses. The first, on the fixed axes case, was focused on obtaining a position control of the robot. The second one, instead, was done on the moving axes case and was more directed towards a problem of stabilization.

The next logical step would be combining these two controls in order to obtain a way to position control the moving axes case while keeping it stable.

The reason while this part could not be included in the thesis was due to lack of time.

### 4.3.4 Expansion to the 3-D case

The most obvious expansion of this work towards the actual realization of the robot of course is the shift from a 2-D analysis to a 3-D one. This requires a lot of work and was thus out of the scope of this thesis, but the information reported in this text should definitely facilitate this operation, since it will be just a matter of making them applicable to a third dimension.

# Chapter 5

# Conclusion

The hope is that this thesis may provide some interesting insights into the subject of automatic controls for both modelling and control, together with maybe providing hints for future developments in the field of robotics.

Although the final goal of this project, the realization of a Ball-Balancing Robot, has been already achieved by several research groups at various universities, the approach that was adopted in this work might offer some alternative points of view on the matter that can maybe facilitate additional improvements for the robot.

The desire of many people is to reach one day the level of technology depicted in our beloved sci-fi movies. Some targets have already been reached, others are still far away. In this huge world of technological progress the ambition is that even this work may play its little part by helping, for example, with the construction of our very own BB-8 droids.

May the *torque* be with you.

# Bibliography


[1] Paolo Biscari et al. *Meccanica razionale*. Vol. 93. Springer, 2015.

[2] Paolo Giuseppe Emilio Bolzern, Riccardo Scattolini, and Nicola Luigi Schiavoni. *Fondamenti di controlli automatici*. McGraw-Hill, 2008.

[3] Frederick William Carter. "On the action of a locomotive driving wheel". In: *Proceedings of the Royal Society of London. Series A, containing papers of a mathematical and physical character* 112.760 (1926), pp. 151–157.

[4] Roberto Diversi. *Slides for Controlli Automatici T-1*. 2019.

[5] Lorenzo Marconi. *Slides for Controlli Automatici T-2*. 2020.

[6] MATLAB. *State Space, Part 2: Pole Placement*. Youtube. 2019. URL: https://www.youtube.com/watch?v=FXSpHy8LvmY.

[7] MATLAB. *State Space, Part 4: What Is LQR control?* Youtube. 2019. URL: https://www.youtube.com/watch?v=E_RDCF0lJx4&t=388s.

[8] Marco Tibaldi. *Progetto di sistemi di controllo*. Pitagora, 1995.

[9] Gianni Vannini. *gettys fisica 1, Meccanica e Termodinamica*. McGraw-Hill, 2015.